



# Convergence analysis of semi-smooth Newton method for mixed FEM approximations of dynamic two-body contact and crack problems

Victor A. Kovtunenکو <sup>a,b</sup> ,\* , Yves Renard <sup>c</sup> 

<sup>a</sup> Department of Mathematics and Scientific Computing, Karl-Franzens University of Graz, NAWI Graz, Heinrichstr. 36, 8010 Graz, Austria

<sup>b</sup> Lavrentyev Institute of Hydrodynamics, Siberian Division of the Russian Academy of Sciences, 630090 Novosibirsk, Russia

<sup>c</sup> INSA Lyon, CNRS, Ecole Centrale de Lyon, Université Claude Bernard Lyon 1, Université Jean Monnet, ICJ UMR5208, LaMCoS UMR5259, 69621 Villeurbanne, France

## ARTICLE INFO

MSC:  
49M15  
70E18  
70F05  
74S05

### Keywords:

Finite-element method  
Newton method  
Convergence analysis  
Two-body problem  
Dynamical contact  
Non-penetrating crack

## ABSTRACT

A class of elastodynamic problems describing contact between two deformable bodies as well as non-penetrating cracks in a single body is considered in the framework of FEM approximation. For time discretization, the Hilber–Hughes–Taylor (HHT- $\alpha$ ) method extending Newmark schemes is incorporated. Using mixed variational formulation of the fully discrete contact problem, a semi-smooth Newton method of solution is provided with the locally super-linear convergence. An equivalent primal–dual active set algorithm validates monotone properties of global convergence for the Newton iterates provided by M-matrix property. Numerical solution of the Signorini contact with rigid obstacle is presented for isotropic body in 2D using benchmark and moving load experiment.

## 1. Introduction

In the framework of computational contact and impact mechanics [1], motion of two deformable elastic bodies coming into contact is studied. As the special case, when contact surfaces for the both bodies coincide in the reference configuration, this setting allows straightforward extension to fracture problems with cracks subjected to non-penetration conditions, see [2]. For the variational theory of elastostatic models of solids and plates with non-penetrating cracks and for the relevant numerical treatment we refer the readers to [3–6] and other works by the authors.

The well-posedness of elastodynamics contact problems is an open question except in one spatial dimension and some particular cases. In several models of the dynamic impact of thin structures, an infinite number of solutions can be exhibited, which can be linked to the fact that the contact surface has its own inertia. To recover or establish the well-posedness, a regularization by viscous damping can be useful, together with the regularization of contact condition. The existence of solutions to the dynamic problems for viscoelastic bodies with frictional contact was proven in [7] with the use of penalization and regularization methods. Contact conditions were formulated in velocities, thus satisfying the persistency condition. Mathematical results on existence for damped evolutionary equations with damped unilateral conditions in case of viscoelastic materials were obtained in [8,9]. For

\* Corresponding author at: Department of Mathematics and Scientific Computing, Karl-Franzens University of Graz, NAWI Graz, Heinrichstr. 36, 8010 Graz, Austria.

E-mail addresses: [victor.kovtunenکو@uni-graz.at](mailto:victor.kovtunenکو@uni-graz.at) (V.A. Kovtunenکو), [Yves.Renard@insa-lyon.fr](mailto:Yves.Renard@insa-lyon.fr) (Y. Renard).

<https://doi.org/10.1016/j.cam.2025.116722>

Received 17 October 2024; Received in revised form 27 January 2025

Available online 12 May 2025

0377-0427/© 2025 The Author(s). Published by Elsevier B.V. This is an open access article under the CC BY license (<http://creativecommons.org/licenses/by/4.0/>).

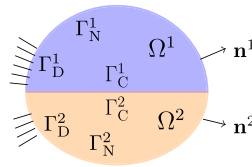


Fig. 1. Example of two body contact in 2D.

solvability of the elastodynamic problem for the crack with a modified contact law see [10]. The abstract theory of evolutionary variational-hemivariational inequalities with applications to dynamic viscoelastic contact mechanics is developing in the works by [11,12].

For the discretization of dynamical contact problems by finite element method (FEM) we refer to [13,14]. The space semi-discretization is ill-posed in the sense that it has an infinite number of solutions corresponding to a choice of the restitution at impact of each contact node. Standard schemes are not stable with respect to mechanical energy and finally blow up rapidly for small time steps. The instability of time-discretization is partially due to violation of the discrete persistency condition. There are known stabilization methods of a restitution coefficient [15] and mass redistribution [13,16]. For energy-consistent methods using penalization we cite [17,18]. Nitsche’s method [19–21] is consistent and converges optimally, hence has better approximation properties than a penalty method. In [22], an unbiased formulation was suggested for bodies which are expected to come into contact in the same way without master and slave surfaces. We refer also to [23] for the relevant methods of boundary elements, and to [24] for domain decomposition.

The discrete problem implies a Linear Complementarity Problem (LCP), which has been studied extensively in the literature with respect to numerical algorithms such as well-established pivoting methods [25]. It is known that, for large number of constrained unknowns, the classical LCP-methods require a large number of iterations. Interior-point and semi-smooth algorithms are the most efficient and robust iterative algorithms with a rather small number of required iterations. In comparison to interior point methods, the semi-smooth Newton strategy determines not an approximate, but the exact solution of the discrete problem. For comprehensive comparisons of the semi-smooth and LCP algorithms we refer the reader to [26,27].

To solve efficiently variational inequalities stemming from complementarity conditions, a semi-smooth Newton method was proposed in [28,29] and other works. It is based on a generalized gradient of non-smooth merit functions, in particular, the minimum-based function. For globalization, Newton iterates can be implemented on primal–dual active sets (PDAS). The application of generalized Newton’s methods for solution of contact and frictional problems in mechanics can be found in [30], and for crack problems with non-penetration conditions in [31,32]. The PDAS strategy was applied to dynamic frictional contact problems in [33] within an energy conserving framework based on the shifted midpoint, and in [34] using the implicit second-order midpoint rule, however, without analysis of convergence properties.

In this work, we formulate the elastodynamic contact problem in Section 2, and introduce its mixed FEM approximation in Section 3. For temporal discretization, we apply the Hilber–Hughes–Taylor method [35] called HHT- $\alpha$  as commonly adopted in the literature (see e.g. [36]). Following [37] our notation extends the schemes of Newmark family given by two weight parameters  $\gamma$  and  $\beta$ , which are considered here as the particular case of HHT- $\alpha$  when the parameter  $\alpha = 1$ . In benchmarks by compression and release, spurious oscillations in the energy are suppressed when using  $\gamma$ -damped as well as  $\alpha$ -damped schemes. Focusing on convergence analysis, in Section 4 we prove rigorously that Newton iterates converge to the fully discrete solution locally with a super-linear rate provided by the M-property of system matrix. We formulate the semi-smooth Newton iteration in the equivalent form of PDAS algorithm, then justify theoretically and validate numerically monotone properties of its global convergence for arbitrary initialization and various parameters  $\alpha$  and  $\gamma, \beta$ . Motivated by railway applications [38], in Section 5 we compute the loop motion of a two-dimensional isotropic body compressed by a rigid obstacle under a moving load and for the corresponding symmetric crack problem.

## 2. Setting of the problem

We consider a system of two deformable elastic bodies coming into contact with each other. Example of the two-body contact geometry is presented in 2D in Fig. 1. For notational convenience, index  $i$  is used to represent in unified way the first body as  $i = 1$ , or the second body as  $i = 2$ , respectively. Let  $\Omega^i$  be the domain in  $\mathbb{R}^d$ , with  $d = 2$  or  $d = 3$ , occupied by the  $i$ th body in the reference configuration. We suppose that the boundary  $\partial\Omega^i$  is Lipschitz continuous and has an outward unit normal vector  $\mathbf{n}^i$ . Let  $\partial\Omega^i$  consist of three mutually non-overlapping parts  $\Gamma_D^i, \Gamma_N^i$  and  $\Gamma_C^i$ . Each body is clamped on the Dirichlet boundary  $\Gamma_D^i$ , and on the Neumann boundary  $\Gamma_N^i$  it is assumed to be free of stress for the sake of simplicity. Whereas a portion of the boundary  $\Gamma_C^i$  of the  $i$ th body is a candidate for contact surface. This means that the actual surface on which the bodies come into contact with each other is unknown in advance and corresponds one-to-one to both  $\Gamma_C^1$  and  $\Gamma_C^2$ . Furthermore,  $t \in [0, T)$  stands for a time with the prescribed final time  $T > 0$ . We denote for short by  $\Omega_T^i = (0, T) \times \Omega^i$  the cylinder, and similarly by  $\Gamma_{DT}^i = (0, T) \times \Gamma_D^i, \Gamma_{NT}^i = (0, T) \times \Gamma_N^i$  its surface portions.

Relatively to the fixed spatial frame, displacements of the bodies can be represented by the pair  $\mathbf{u} = (\mathbf{u}^1, \mathbf{u}^2)$  in the multi-domain  $\Omega = \Omega^1 \cup \Omega^2$ , where  $\mathbf{u}^i$  is the displacement field of the  $i$ th body. Small strain assumption is made, such that the linearized strain tensor field is represented by

$$\boldsymbol{\varepsilon}(\mathbf{u}^i) = \frac{1}{2} (\nabla \mathbf{u}^i + (\nabla \mathbf{u}^i)^T), \tag{2.1}$$

with the transposed gradient, and the stress tensor field is given by Hooke’s law:

$$\sigma(\mathbf{u}^i) = \mathbf{A}^i \varepsilon(\mathbf{u}^i) \quad \text{in } \Omega_T^i \tag{2.2}$$

where  $\mathbf{A}^1$  and  $\mathbf{A}^2$  are the fourth order symmetric elasticity tensors having the usual uniform ellipticity and boundedness properties. Each body is subjected to the volume force  $\mathbf{f}^i$  prescribed in  $\Omega_T^i$ .

The dynamic two-body contact problem consists in finding the displacement field  $\mathbf{u} : [0, T) \times \Omega \mapsto \mathbb{R}^d$  satisfying constitutive Eqs. (2.1) and (2.2), the equation of motion

$$\rho^i \dot{\mathbf{u}}^i - \operatorname{div} \sigma(\mathbf{u}^i) = \mathbf{f}^i \quad \text{in } \Omega_T^i, \tag{2.3}$$

where density of the elastic material denoted by  $\rho^i$  is supposed to be constant, and the initial conditions:

$$\mathbf{u}^i(0, \cdot) = \mathbf{u}_0^i, \quad \dot{\mathbf{u}}^i(0, \cdot) = \dot{\mathbf{u}}_0^i \quad \text{in } \Omega^i. \tag{2.4}$$

Here the notation  $\dot{\mathbf{u}}$  stands for the velocity and  $\ddot{\mathbf{u}}$  for acceleration;  $\mathbf{u}_0^i$  is the initial displacement and  $\dot{\mathbf{u}}_0^i$  is the initial velocity of the  $i$ th body. Eqs. (2.1)–(2.4) are endowed with the mixed Dirichlet–Neumann boundary conditions:

$$\mathbf{u}^i = \mathbf{0} \quad \text{on } \Gamma_{DT}^i, \quad \sigma(\mathbf{u}^i) \mathbf{n}^i = \mathbf{0} \quad \text{on } \Gamma_{NT}^i, \tag{2.5}$$

and contact conditions described hereafter.

Let  $\Gamma_C$  be a Lipschitz continuous oriented surface in  $\mathbb{R}^d$  with an outward unit normal vector  $\mathbf{n}$ , and  $\Gamma_{CT} = (0, T) \times \Gamma_C$ . For any displacement field  $\mathbf{v}$  defined on the surface we adopt the orthogonal decomposition:

$$\mathbf{v} = v_n \mathbf{n} + \mathbf{v}_T, \quad v_n = \mathbf{v} \cdot \mathbf{n} \quad \text{on } \Gamma_C, \tag{2.6}$$

where “ $\cdot$ ” denotes the scalar product of vectors (or tensor contraction) and  $\mathbf{v}_T$  are tangential components of  $\mathbf{v}$ . Let us assume a bijective mapping (diffeomorphism)

$$\Pi^i : \Gamma_C^i \mapsto \Gamma_C, \tag{2.7}$$

associating each point of the boundary portion  $\Gamma_C^i$  of the  $i$ th body to a point of the contact surface  $\Gamma_C$  such that the Jacobian determinant of the transformation  $J^i > 0$ . Then we can define the relative jump of fields across the contact surface:

$$\llbracket \mathbf{u} \rrbracket = \mathbf{u}^1 \circ \Pi^1 - \mathbf{u}^2 \circ \Pi^2.$$

We choose the direction of normal  $\mathbf{n}$  such that the opening is non-negative:

$$\llbracket u_n \rrbracket = (\mathbf{u}^1 \circ \Pi^1 - \mathbf{u}^2 \circ \Pi^2) \cdot \mathbf{n} \geq 0. \tag{2.8}$$

Using (2.6) and (2.7) such that the transformed stress field is decomposed as

$$\begin{cases} J^i(\sigma(\mathbf{u}^i) \mathbf{n}^i) \circ \Pi^i = \sigma_n(\mathbf{u}^i) \mathbf{n} + (J^i(\sigma(\mathbf{u}^i) \mathbf{n}^i) \circ \Pi^i)_T, \\ \sigma_n(\mathbf{u}^i) = (J^i(\sigma(\mathbf{u}^i) \mathbf{n}^i) \circ \Pi^i) \cdot \mathbf{n} \quad \text{on } \Gamma_C, \end{cases}$$

the two-body contact is friction-free:

$$(J^i(\sigma(\mathbf{u}^i) \mathbf{n}^i) \circ \Pi^i)_T = \mathbf{0} \quad \text{on } \Gamma_{CT}, \tag{2.9}$$

and verifies the following unilateral conditions owing to non-penetration (2.8):

$$\llbracket u_n \rrbracket \geq 0, \quad \sigma_n(\mathbf{u}) \leq 0, \quad \sigma_n(\mathbf{u}) \llbracket u_n \rrbracket = 0 \quad \text{on } \Gamma_{CT}. \tag{2.10}$$

The normal stress across the contact surface:

$$\sigma_n(\mathbf{u}) = -(J^1(\sigma(\mathbf{u}^1) \mathbf{n}^1) \circ \Pi^1) \cdot \mathbf{n} = (J^2(\sigma(\mathbf{u}^2) \mathbf{n}^2) \circ \Pi^2) \cdot \mathbf{n} \tag{2.11}$$

is continuous ( $\llbracket \sigma_n(\mathbf{u}) \rrbracket = 0$ ), and the negative sign corresponds to compression.

**Example 2.1.** As in example Fig. 1, let the contact surfaces  $\Gamma_C^i = \Gamma_C$  coincide such that  $\Pi^i$  is the identity transformation and  $J^i = 1$ . In this case, choice of the normal direction  $\mathbf{n} = -\mathbf{n}^1 = \mathbf{n}^2$  corresponds to the positive sign in (2.8). The normal jump in (2.8) and boundary stresses in (2.9) and (2.11) are:

$$\llbracket u_n \rrbracket = (\mathbf{u}^1 - \mathbf{u}^2) \cdot \mathbf{n}, \quad \sigma_n(\mathbf{u}) = \sigma(\mathbf{u}^i) \mathbf{n} \cdot \mathbf{n}, \quad \sigma_T(\mathbf{u}^i) = \sigma(\mathbf{u}^i) \mathbf{n} - \sigma_n(\mathbf{u}) \mathbf{n}.$$

**Remark 2.1.** Within Example 2.1, if the transmission conditions:

$$\llbracket u_n \rrbracket = 0, \quad \llbracket \sigma_n(\mathbf{u}) \rrbracket = 0 \quad \text{on } \Sigma_T = (0, T) \times \Sigma$$

hold on a portion  $\Sigma$  of contact boundary  $\Gamma_C$ , then its complement:

$$\llbracket u_n \rrbracket \geq 0, \quad \sigma_n(\mathbf{u}) \leq 0, \quad \sigma_n(\mathbf{u}) \llbracket u_n \rrbracket = 0 \quad \text{on } \Gamma_{CT} \setminus \Sigma_T$$

implies a non-penetrating crack according to the description of [2].

2.1. Variational formulation

Let us introduce the Hilbert space:

$$\mathbf{V} = \{ \mathbf{v} = (\mathbf{v}^1, \mathbf{v}^2) \in H^1(\Omega^1)^d \times H^1(\Omega^2)^d \mid \mathbf{v}^i = \mathbf{0} \text{ a.e. } \Gamma_D^i \}$$

accounting for the Dirichlet boundary condition in (2.5), and the Bochner space

$$\mathbf{W} = \{ \mathbf{v} \in L^2(0, T; \mathbf{V}), \quad \dot{\mathbf{v}} = (\dot{\mathbf{v}}^1, \dot{\mathbf{v}}^2) \in L^2(0, T; L^2(\Omega^d)) \},$$

where  $L^2(\Omega) = L^2(\Omega^1) \times L^2(\Omega^2)$ . We define the convex cone  $\mathbf{K}$  of admissible displacements which satisfy the non-penetration (2.8) on the contact surface:

$$\mathbf{K} = \{ \mathbf{v} \in \mathbf{V} \mid \llbracket v_n \rrbracket \geq 0 \text{ a.e. } \Gamma_C \}.$$

Suppose that the initial fields in (2.4) satisfy  $\mathbf{u}_0 = (\mathbf{u}_0^1, \mathbf{u}_0^2) \in \mathbf{K}$ , and that  $\dot{\mathbf{u}}_0 = (\dot{\mathbf{u}}_0^1, \dot{\mathbf{u}}_0^2) \in L^2(\Omega)^d$ . Suppose also that the body force  $\mathbf{f} = (\mathbf{f}^1, \mathbf{f}^2) \in C([0, T]; L^2(\Omega)^d)$ , which imply that  $\mathbf{f}$  belongs to  $L^2((0, T) \times \Omega)^d$ .

For smooth fields  $\mathbf{u}^i$  and  $\mathbf{v}^i$  in the  $i$ th body the Green's formula holds:

$$- \int_{\Omega^i} \operatorname{div} \boldsymbol{\sigma}(\mathbf{u}^i) \cdot \mathbf{v}^i \, d\mathbf{x} = \int_{\Omega^i} \boldsymbol{\sigma}(\mathbf{u}^i) : \boldsymbol{\varepsilon}(\mathbf{v}^i) \, d\mathbf{x} - \int_{\partial\Omega^i} \boldsymbol{\sigma}(\mathbf{u}^i) \mathbf{n}^i \cdot \mathbf{v}^i \, d\Gamma,$$

where notation “:” stands for the tensor double contraction. Applying on the contact surface the one-to-one transformation  $\Pi^i : \Gamma_C^i \mapsto \Gamma_C$  from (2.6) and (2.7) yields the sum

$$\begin{aligned} & - \int_{\Omega} \operatorname{div} \boldsymbol{\sigma}(\mathbf{u}) \cdot \mathbf{v} \, d\mathbf{x} = \int_{\Omega} \boldsymbol{\sigma}(\mathbf{u}) : \boldsymbol{\varepsilon}(\mathbf{v}) \, d\mathbf{x} - \sum_{i=1}^2 \int_{\Gamma_D^i \cup \Gamma_N^i} \boldsymbol{\sigma}(\mathbf{u}^i) \mathbf{n}^i \cdot \mathbf{v}^i \, d\Gamma \\ & + \sum_{i=1}^2 \int_{\Gamma_C} (J^i(\boldsymbol{\sigma}(\mathbf{u}^i) \mathbf{n}^i) \circ \Pi^i)_\Gamma \cdot (\mathbf{v}^i \circ \Pi^i)_\Gamma \, d\Gamma + \int_{\Gamma_C} \llbracket \sigma_n(\mathbf{u}) v_n \rrbracket \, d\Gamma. \end{aligned} \tag{2.12}$$

Denote by  $\rho = (\rho^1, \rho^2)$  the density in  $\Omega$  and by  $\Omega_T = (0, T) \times \Omega$  the time-space domain. The substitution of the equation of motion (2.3) and boundary conditions (2.5), (2.9) and (2.10) into (2.12) tested by  $\mathbf{v} - \mathbf{u}$  and integrated over  $t \in (0, T)$  yields

$$\begin{aligned} & \int_{\Omega_T} (\rho \ddot{\mathbf{u}} - \mathbf{f}) \cdot (\mathbf{v} - \mathbf{u}) \, d\mathbf{x} dt + \int_{\Omega_T} \boldsymbol{\sigma}(\mathbf{u}) : \boldsymbol{\varepsilon}(\mathbf{v} - \mathbf{u}) \, d\mathbf{x} dt \\ & = - \int_{\Gamma_{CT}} \sigma_n(\mathbf{u}) \llbracket v_n \rrbracket \, d\Gamma dt. \end{aligned} \tag{2.13}$$

Upon integrating (2.13) by parts over time using initial conditions (2.4) and

$$\int_0^T \rho \ddot{\mathbf{u}} \cdot \mathbf{v} \, dt = - \int_0^T \rho \dot{\mathbf{u}} \cdot \dot{\mathbf{v}} \, dt + \rho \dot{\mathbf{u}}(T, \cdot) \cdot \mathbf{v}(T, \cdot) - \rho \dot{\mathbf{u}}(0, \cdot) \cdot \mathbf{v}(0, \cdot),$$

a weak formulation of the problem (2.1)–(2.11) reads as:

$$\left\{ \begin{array}{l} \text{Find } \mathbf{u} \in \mathbf{W}, \mathbf{u}(t, \cdot) \in \mathbf{K} \text{ for } t \in (0, T), \mathbf{u}(0, \cdot) = \mathbf{u}_0, \text{ such that:} \\ - \int_{\Omega_T} \rho \dot{\mathbf{u}} \cdot (\dot{\mathbf{v}} - \dot{\mathbf{u}}) \, d\mathbf{x} dt + \int_{\Omega_T} \boldsymbol{\sigma}(\mathbf{u}) : \boldsymbol{\varepsilon}(\mathbf{v} - \mathbf{u}) \, d\mathbf{x} dt \\ \geq \int_{\Omega} \rho \dot{\mathbf{u}}_0 \cdot (\mathbf{v}(0, \cdot) - \mathbf{u}_0) \, d\mathbf{x} + \int_{\Omega_T} \mathbf{f} \cdot (\mathbf{v} - \mathbf{u}) \, d\mathbf{x} dt \\ \text{for all } \mathbf{v} \in \mathbf{W}, \mathbf{v}(t, \cdot) \in \mathbf{K}, \text{ and } \mathbf{v} = \mathbf{u} \text{ for } t \geq T - \zeta \text{ with } \zeta > 0. \end{array} \right. \tag{2.14}$$

Note that within the function space  $\mathbf{V}$  the boundary trace  $\boldsymbol{\sigma}(\mathbf{u}^i) \mathbf{n}^i$  can be defined at  $\partial\Omega^i$  as  $H^{-1/2}$ -distribution only. Therefore, it follows

**Remark 2.2.** Let  $\mathbf{u}$  be a sufficiently regular solution to the variational problem (2.14), then it solves the initial boundary value problem (2.1)–(2.11).

For fixed  $t \in [0, T]$ , the mechanical energy associated with the solution  $\mathbf{u}$  of the problem (2.14) is defined as

$$E(t) = \frac{1}{2} \int_{\Omega} \rho |\dot{\mathbf{u}}|^2 \, d\mathbf{x} + \frac{1}{2} \int_{\Omega} \boldsymbol{\sigma}(\mathbf{u}) : \boldsymbol{\varepsilon}(\mathbf{u}) \, d\mathbf{x}, \tag{2.15}$$

where  $|\cdot|$  is the vector  $\ell^2$ -norm. Formally testing (2.12) with  $\mathbf{v} = \dot{\mathbf{u}}$ , after integration by parts with the boundary conditions (2.5), (2.9) and (2.10) yields similarly to (2.13) the identity:

$$\int_{\Omega} (\rho \ddot{\mathbf{u}} - \mathbf{f}) \cdot \dot{\mathbf{u}} \, d\mathbf{x} + \int_{\Omega} \boldsymbol{\sigma}(\mathbf{u}) : \boldsymbol{\varepsilon}(\dot{\mathbf{u}}) \, d\mathbf{x} = - \int_{\Gamma_C} \sigma_n(\mathbf{u}) \llbracket \dot{u}_n \rrbracket \, d\Gamma.$$

If  $\dot{\mathbf{u}}$  is continuous in time, then the persistency condition  $\sigma_n(\mathbf{u})\llbracket\dot{u}_n\rrbracket = 0$  holds on  $\Gamma_{CT}$ . Upon differentiating (2.15) with respect to time we end up with:

$$\frac{d}{dt} E(t) - \int_{\Omega} \mathbf{f} \cdot \dot{\mathbf{u}} \, d\mathbf{x} = 0. \tag{2.16}$$

As a consequence of (2.16), we get

**Remark 2.3.** If the body force  $\mathbf{f}$  vanishes and the persistency condition is valid, then energy conservation holds:  $E(t) = E(0)$  for all  $t \in [0, T]$ .

### 3. Discretization of the variational problem

Let  $\mathcal{T}_h^i$  be a family of triangulations of the domain  $\Omega^i$ . The mesh size  $h = \max_{K \in \mathcal{T}_h^i} h_K$  where  $h_K$  is the diameter of set  $K$ . The triangulation is supposed regular and conformal to the subdivisions of the boundaries into  $\Gamma_D^i$ ,  $\Gamma_N^i$  and  $\Gamma_C^i$ , which means that a face of an element  $K \in \mathcal{T}_h^i$  is not allowed to have simultaneous non-empty intersection with more than one part of the subdivision. We introduce the family of finite-dimensional vector spaces  $\mathbf{V}_h = \mathbf{V}_h^1 \times \mathbf{V}_h^2$  indexed by  $h > 0$  and build by piecewise on  $\mathcal{T}_h^i$  polynomials of degree  $p \in \mathbb{N}$ :

$$\mathbf{V}_h^i = \{ \mathbf{v}_h^i \in C^0(\overline{\Omega^i}) \mid \mathbf{v}_h^i|_K \in (\mathbb{P}_p(K))^d \text{ for all } K \in \mathcal{T}_h^i, \mathbf{v}_h^i = \mathbf{0} \text{ on } \Gamma_D^i \}.$$

Let us assume a discrete counterpart of the bijection  $\Pi^i$  in (2.7):

$$\Pi_h^i : K \cap \Gamma_C^i \mapsto \Gamma_C^h \text{ for all } K \in \mathcal{T}_h^i,$$

where  $\Gamma_C^h$  is a finite set of  $N_C^h \in \mathbb{N}$  nodes belonging to the contact surface  $\Gamma_C$ . The discretized non-penetration condition (2.8) is

$$\llbracket u_{hn} \rrbracket = (\mathbf{u}_h^1 \circ \Pi_h^1 - \mathbf{u}_h^2 \circ \Pi_h^2) \cdot \mathbf{n} \geq 0 \text{ on } \Gamma_C^h. \tag{3.1}$$

Complementary to (3.1) we introduce the Lagrange multiplier  $\lambda_h : [0, T] \mapsto \mathbb{R}^{N_C^h}$  which verifies the complementarity conditions according to (2.10):

$$\llbracket u_{hn} \rrbracket \geq 0, \quad \lambda_h \leq 0, \quad \lambda_h \llbracket u_{hn} \rrbracket = 0 \text{ on } \Gamma_{CT}^h, \tag{3.2}$$

where  $\Gamma_{CT}^h = (0, T) \times \Gamma_C^h$ . If the normal stress  $\sigma_n(\mathbf{u})$  in (2.11) is regular, then  $\lambda_h$  in (3.2) implies its FEM approximation.

The semi-discretized in space variational problem (2.14) reads:

$$\left\{ \begin{array}{l} \text{Find } \mathbf{u}_h : (0, T) \mapsto \mathbf{V}_h, \mathbf{u}_h(0, \cdot) = \mathbf{u}_{0h}, \llbracket u_{hn} \rrbracket \geq 0 \text{ on } \Gamma_{CT}^h : \\ \int_{\Omega_T} \rho \ddot{\mathbf{u}}_h \cdot (\mathbf{v}_h - \mathbf{u}_h) \, d\mathbf{x}dt + \int_{\Omega_T} \boldsymbol{\sigma}(\mathbf{u}_h) : \boldsymbol{\varepsilon}(\mathbf{v}_h - \mathbf{u}_h) \, d\mathbf{x}dt \\ \geq \int_{\Omega_T} \mathbf{f} \cdot (\mathbf{v}_h - \mathbf{u}_h) \, d\mathbf{x}dt \\ \text{for all } \mathbf{v}_h \in C^0([0, T]; \mathbf{V}_h) \text{ with } \llbracket v_{hn} \rrbracket \geq 0 \text{ on } \Gamma_{CT}^h, \end{array} \right. \tag{3.3}$$

where  $\mathbf{u}_{0h}$  (respectively  $\dot{\mathbf{u}}_{0h}$ ) is an approximation in  $\mathbf{V}_h$  of the initial displacement  $\mathbf{u}_0$  (respectively the initial velocity  $\dot{\mathbf{u}}_0$ ).

**Remark 3.1.** We assume  $\llbracket u_n \rrbracket \geq 0$  a.e.  $\Gamma_C$  follows that  $\llbracket u_{hn} \rrbracket \geq 0$  on  $\Gamma_C^h$ . The semi-discrete variational problem (3.3) is consistent in the following sense: if the solution  $\mathbf{u}$  of (2.14) is sufficiently smooth, then it satisfies also (3.3).

Indeed, from the Green’s formula (2.13) hold for smooth  $\mathbf{u}$ , using the complementarity conditions (2.10) we infer the identity:

$$\int_{\Omega_T} \rho \ddot{\mathbf{u}} \cdot \mathbf{u} \, d\mathbf{x}dt + \int_{\Omega_T} \boldsymbol{\sigma}(\mathbf{u}) : \boldsymbol{\varepsilon}(\mathbf{u}) \, d\mathbf{x}dt = \int_{\Omega_T} \mathbf{f} \cdot \mathbf{u} \, d\mathbf{x}dt,$$

and the variational equation hold for all  $\mathbf{v} \in \mathbf{V}$ :

$$\int_{\Omega_T} \rho \ddot{\mathbf{u}} \cdot \mathbf{v} \, d\mathbf{x}dt + \int_{\Omega_T} \boldsymbol{\sigma}(\mathbf{u}) : \boldsymbol{\varepsilon}(\mathbf{v}) \, d\mathbf{x}dt = \int_{\Omega_T} \mathbf{f} \cdot \mathbf{v} \, d\mathbf{x}dt - \int_{\Gamma_{CT}} \sigma_n(\mathbf{u}) \llbracket v_n \rrbracket \, d\Gamma dt.$$

Using  $\sigma_n(\mathbf{u}) \leq 0$  and testing  $\mathbf{v} = \mathbf{v}_h$  yields (3.3) with  $\mathbf{u}_h$  replaced by  $\mathbf{u}$ .

For integer  $N$ , let  $\tau = T/N$  be the step size, and consider a uniform discretization of the time interval  $[0, T]$  with points  $t^m = m\tau$  for  $m = 0, \dots, N$ . Hereafter we denote by  $\mathbf{u}_h^m$  (respectively  $\dot{\mathbf{u}}_h^m$  and  $\ddot{\mathbf{u}}_h^m$ ) the discretized displacement (respectively velocity and acceleration) at time  $t^m$ , and weighted sum with parameter  $\alpha > 0$ :

$$\mathbf{v}_h^{m+\alpha} = \alpha \mathbf{v}_h^{m+1} + (1 - \alpha) \mathbf{v}_h^m.$$

Respectively, the semi-discrete force  $\mathbf{f}^m = \mathbf{f}(t^m, \cdot)$  and the Lagrange multiplier  $\lambda_h^m = \lambda_h(t^m)$  for  $m = 0, \dots, N$  and intermediate time steps  $m + \alpha$ .

It is well-known that a standard scheme such as Crank–Nicolson is not stable since the energy may start oscillate and blow up by decreasing step size. Therefore, we apply a most general Hilber–Hughes–Taylor (HHT) implicit  $\alpha$ -method following [37], which extends the Newmark scheme with prescribed parameters  $\gamma \in [0, 1]$  and  $\beta \in [0, 0.5]$ . For  $m \geq 0$  we perform the fully discrete variational problem (3.3) in mixed formulation owing to (3.2):

$$\left\{ \begin{array}{l} \text{Find } \mathbf{u}_h^{m+1}, \dot{\mathbf{u}}_h^{m+1}, \ddot{\mathbf{u}}_h^{m+1} \in \mathbf{V}_h \text{ and } \lambda_h^{m+\alpha} \in \mathbb{R}^{N_C^h} \text{ such that:} \\ \mathbf{u}_h^{m+1} = \mathbf{u}_h^m + \tau \dot{\mathbf{u}}_h^m + \frac{\tau^2}{2} \ddot{\mathbf{u}}_h^{m+2\beta}, \\ \dot{\mathbf{u}}_h^{m+1} = \dot{\mathbf{u}}_h^m + \tau \ddot{\mathbf{u}}_h^{m+\gamma}, \\ \int_{\Omega} \rho \ddot{\mathbf{u}}_h^{m+1} \cdot \mathbf{v}_h \, d\mathbf{x} + \int_{\Omega} \boldsymbol{\sigma}(\mathbf{u}_h^{m+\alpha}) : \boldsymbol{\varepsilon}(\mathbf{v}_h) \, d\mathbf{x} + \lambda_h^{m+\alpha} \cdot \llbracket v_{hn} \rrbracket \\ = \int_{\Omega} \mathbf{f}^{m+\alpha} \cdot \mathbf{v}_h \, d\mathbf{x} \quad \text{for all } \mathbf{v}_h \in \mathbf{V}_h, \\ \llbracket u_{hn}^{m+\alpha} \rrbracket \geq 0, \quad \lambda_h^{m+\alpha} \leq 0, \quad \lambda_h^{m+\alpha} \llbracket u_{hn}^{m+\alpha} \rrbracket = 0 \quad \text{on } \Gamma_C^h, \end{array} \right. \tag{3.4}$$

with initial fields  $\mathbf{u}_h^0 = \mathbf{u}_{0h}$  and  $\dot{\mathbf{u}}_h^0 = \dot{\mathbf{u}}_{0h}$ . The acceleration may be initialized through solution  $\ddot{\mathbf{u}}_h^0$  of the system:

$$\left\{ \begin{array}{l} \int_{\Omega} (\rho \ddot{\mathbf{u}}_h^0 - \mathbf{f}^0) \cdot \mathbf{v}_h \, d\mathbf{x} + \int_{\Omega} \boldsymbol{\sigma}(\mathbf{u}_h^0) : \boldsymbol{\varepsilon}(\mathbf{v}_h) \, d\mathbf{x} + \lambda_h^0 \cdot \llbracket v_{hn} \rrbracket = 0 \quad \text{for all } \mathbf{v}_h \in \mathbf{V}_h, \\ \llbracket u_{hn}^0 \rrbracket \geq 0, \quad \lambda_h^0 \leq 0, \quad \lambda_h^0 \llbracket u_{hn}^0 \rrbracket = 0 \quad \text{on } \Gamma_C^h. \end{array} \right.$$

**Remark 3.2.** The HHT- $\alpha$  system (3.4) for  $\alpha = 1$  turns into the scheme of Newmark family. The HHT- $\alpha$  scheme corresponds to the special choice of parameters  $\gamma = 1/2 + \tilde{\alpha}$  and  $\beta = (1 + \tilde{\alpha})^2/4$ , where  $\tilde{\alpha} = 1 - \alpha$ . It yields unconditional stability for  $0 < \tilde{\alpha} < 1/3$  and second order consistency for linear elasticity (see [36,39]) and turns into the Crank–Nicolson scheme as  $\alpha = 1$  ( $\tilde{\alpha} = 0$ ).

### 3.1. Well-posedness and stability of the fully discrete formulation

We first recall estimates for  $\mathbf{v}_h \in \mathbf{V}_h$  provided by uniform ellipticity and boundedness properties of the elasticity tensor in (2.2). There exist constants  $C_E, C_K, C_I > 0$ , which are independent of the mesh size  $h$ , such that

$$\|\boldsymbol{\varepsilon}(\mathbf{v}_h)\|_{0,\Omega} \leq \|\nabla \mathbf{v}_h\|_{0,\Omega}, \quad \|\boldsymbol{\sigma}(\mathbf{v}_h)\|_{0,\Omega} \leq C_E \|\nabla \mathbf{v}_h\|_{0,\Omega}, \tag{3.5}$$

in the  $L^2(\Omega)$ -norm  $\|\cdot\|_{0,\Omega}$ , and Korn’s and Poincaré’s inequalities yield

$$\int_{\Omega} \boldsymbol{\sigma}(\mathbf{v}_h) : \boldsymbol{\varepsilon}(\mathbf{v}_h) \, d\mathbf{x} \geq C_K \|\mathbf{v}_h\|_{1,\Omega}^2, \quad \|\mathbf{v}_h\|_{1,\Omega}^2 = \|\mathbf{v}_h\|_{0,\Omega}^2 + \|\nabla \mathbf{v}_h\|_{0,\Omega}^2, \tag{3.6}$$

with respect to the  $H^1(\Omega)$ -norm  $\|\cdot\|_{1,\Omega}$ . Suppose that the mesh  $\mathcal{T}_h^i$  is quasi-uniform, then the inverse inequality holds:

$$\|\mathbf{v}_h\|_{0,\Omega} \geq C_I h \|\mathbf{v}_h\|_{1,\Omega}. \tag{3.7}$$

**Proposition 3.1.** *At each time-step  $m$ , the fully discrete mixed variational problem (3.4) admits one unique solution.*

**Proof.** Reducing the unknowns  $\dot{\mathbf{u}}_h^{m+1}$  and  $\ddot{\mathbf{u}}_h^{m+1}$  such that

$$\left\{ \begin{array}{l} \dot{\mathbf{u}}_h^{m+1} = \frac{\gamma}{\beta\tau} (\mathbf{u}_h^{m+1} - \mathbf{u}_h^m) + (1 - \frac{\gamma}{\beta}) \dot{\mathbf{u}}_h^m + \tau (1 - \frac{\gamma}{2\beta}) \ddot{\mathbf{u}}_h^m, \\ \ddot{\mathbf{u}}_h^{m+1} = \frac{1}{\beta\tau^2} (\mathbf{u}_h^{m+1} - \mathbf{u}_h^m) - \frac{1}{\beta\tau} \dot{\mathbf{u}}_h^m + (1 - \frac{1}{2\beta}) \ddot{\mathbf{u}}_h^m, \end{array} \right. \tag{3.8}$$

the HHT system (3.4) can be rewritten explicitly:

$$\left\{ \begin{array}{l} \text{Find } (\mathbf{u}_h^{m+\alpha}, \lambda_h^{m+\alpha}) \in \mathbf{V}_h \times \mathbb{R}^{N_C^h} \text{ such that:} \\ \mathbf{A}_\tau(\mathbf{u}_h^{m+\alpha}, \mathbf{v}_h) + \lambda_h^{m+\alpha} \cdot \llbracket v_{hn} \rrbracket = \mathbf{F}_\tau^m(\mathbf{v}_h) \quad \text{for all } \mathbf{v}_h \in \mathbf{V}_h, \\ \llbracket u_{hn}^{m+\alpha} \rrbracket \geq 0, \quad \lambda_h^{m+\alpha} \leq 0, \quad \lambda_h^{m+\alpha} \llbracket u_{hn}^{m+\alpha} \rrbracket = 0 \quad \text{on } \Gamma_C^h, \end{array} \right. \tag{3.9}$$

with the bilinear operator  $\mathbf{A}_\tau : \mathbf{V}_h \times \mathbf{V}_h \mapsto \mathbb{R}$  in the left-hand side:

$$\mathbf{A}_\tau(\mathbf{u}_h, \mathbf{v}_h) = \int_{\Omega} \left( \frac{\rho}{\alpha\beta\tau^2} \mathbf{u}_h \cdot \mathbf{v}_h + \boldsymbol{\sigma}(\mathbf{u}_h) : \boldsymbol{\varepsilon}(\mathbf{v}_h) \right) d\mathbf{x}, \tag{3.10}$$

and the linear operator  $\mathbf{F}_\tau^m : \mathbf{V}_h \mapsto \mathbb{R}$  in the right-hand side of (3.9):

$$\mathbf{F}_\tau^m(\mathbf{v}_h) = \int_{\Omega} \left[ \mathbf{f}^{m+\alpha} + \frac{\rho}{\beta\tau^2} \left( \frac{1}{\alpha} \mathbf{u}_h^m + \tau \dot{\mathbf{u}}_h^m + \tau^2 \left( \frac{1}{2} - \beta \right) \ddot{\mathbf{u}}_h^m \right) \right] \cdot \mathbf{v}_h \, d\mathbf{x}. \tag{3.11}$$

When reducing  $\lambda_h^{m+\alpha}$ , the mixed problem (3.9) yields a variational inequality:

$$\begin{cases} \text{Find } \mathbf{u}_h^{m+\alpha} \in \mathbf{V}_h \text{ with } \llbracket u_{hn}^{m+\alpha} \rrbracket \geq 0 \text{ on } \Gamma_C^h \text{ such that} \\ \mathbf{A}_\tau(\mathbf{u}_h^{m+\alpha}, \mathbf{v}_h - \mathbf{u}_h^{m+\alpha}) \geq \mathbf{F}_\tau^m(\mathbf{v}_h - \mathbf{u}_h^{m+\alpha}) \\ \text{for all } \mathbf{v}_h \in \mathbf{V}_h \text{ with } \llbracket v_{hn} \rrbracket \geq 0 \text{ on } \Gamma_C^h. \end{cases} \tag{3.12}$$

The operator  $\mathbf{A}_\tau$  is bounded due to (3.5) and coercive owing to (3.6) and (3.7):

$$\mathbf{A}_\tau(\mathbf{v}_h, \mathbf{v}_h) \geq \left( \frac{\rho h^2}{\alpha \beta \tau^2} C_1^2 + C_K \right) \|\mathbf{v}_h\|_{1,\Omega}^2. \tag{3.13}$$

Therefore, the Lions–Stampacchia theorem for variational inequalities [40] justifies unique solution to (3.12), hence to (3.4) and (3.9). □

**Remark 3.3.** For the fully implicit scheme as  $\gamma = 1, \beta = 0.5, \alpha = 1$  in (3.4) the following stability estimate holds:

$$E_h^{m+1} - \int_\Omega \mathbf{f}^{m+1} \cdot \mathbf{u}_h^{m+1} \, d\mathbf{x} \leq E_h^m - \int_\Omega \mathbf{f}^{m+1} \cdot \mathbf{u}_h^m \, d\mathbf{x}, \tag{3.14}$$

where the energy is discretized from (2.15):

$$E_h^m = \frac{1}{2} \int_\Omega \rho |\dot{\mathbf{u}}_h^m|^2 \, d\mathbf{x} + \frac{1}{2} \int_\Omega \sigma(\mathbf{u}_h^m) : \varepsilon(\mathbf{u}_h^m) \, d\mathbf{x}, \quad m = 0, \dots, N. \tag{3.15}$$

Indeed, for  $\alpha = 1$  inserting the identity  $\dot{\mathbf{u}}_h^{m+1} = (\dot{\mathbf{u}}_h^{m+1} - \dot{\mathbf{u}}_h^m)/\tau$  and the test function  $\mathbf{v}_h = \mathbf{u}_h^{m+1} - \mathbf{u}_h^m = \tau(\dot{\mathbf{u}}_h^{m+1} + \dot{\mathbf{u}}_h^m)/2$  into (3.4) yields

$$\begin{aligned} & \frac{1}{2} \int_\Omega \rho (\dot{\mathbf{u}}_h^{m+1} - \dot{\mathbf{u}}_h^m) \cdot (\dot{\mathbf{u}}_h^{m+1} + \dot{\mathbf{u}}_h^m) \, d\mathbf{x} - \int_\Omega \mathbf{f}^{m+1} \cdot (\mathbf{u}_h^{m+1} - \mathbf{u}_h^m) \, d\mathbf{x} \\ & + \frac{1}{2} \int_\Omega \sigma(\mathbf{u}_h^{m+1} + \mathbf{u}_h^m) : \varepsilon(\mathbf{u}_h^{m+1} - \mathbf{u}_h^m) \, d\mathbf{x} + \lambda_h^{m+1} \cdot \llbracket u_{hn}^{m+1} \rrbracket \\ & = \lambda_h^{m+1} \cdot \llbracket u_{hn}^m \rrbracket - \frac{1}{2} \int_\Omega \sigma(\mathbf{u}_h^{m+1} - \mathbf{u}_h^m) : \varepsilon(\mathbf{u}_h^{m+1} - \mathbf{u}_h^m) \, d\mathbf{x} \leq 0, \end{aligned}$$

which leads to (3.14) using the notation (3.15).

#### 4. Semi-smooth Newton method for the discretized problem

We introduce a nonlinear merit function  $\Phi : \mathbb{R}^2 \mapsto \mathbb{R}$  arising as the minimum:

$$\Phi(\llbracket u_{hn} \rrbracket, \lambda_h) = \min(\llbracket u_{hn} \rrbracket, -r\lambda_h), \tag{4.1}$$

where  $r > 0$  is an arbitrary constant. Using (4.1) we express (3.9) equivalently as the system of variational and nonlinear equations for  $m \geq 0$ :

$$\begin{cases} \text{Find } (\mathbf{u}_h^{m+\alpha}, \lambda_h^{m+\alpha}) \in \mathbf{V}_h \times \mathbb{R}^{\mathcal{N}_C^h} \text{ such that:} \\ \mathbf{A}_\tau(\mathbf{u}_h^{m+\alpha}, \mathbf{v}_h) + \lambda_h^{m+\alpha} \cdot \llbracket v_{hn} \rrbracket = \mathbf{F}_\tau^m(\mathbf{v}_h) \quad \text{for all } \mathbf{v}_h \in \mathbf{V}_h, \\ \Phi(\llbracket u_{hn}^{m+\alpha} \rrbracket, \lambda_h^{m+\alpha}) = 0 \quad \text{on } \Gamma_C^h. \end{cases} \tag{4.2}$$

Whilst the minimum function is not differentiable at zero, for solution of (4.2) we employ a concept of semi-smooth functions from [41].

**Lemma 4.1.** Define a generalized gradient  $\nabla\Phi : \mathbb{R}^2 \mapsto \mathbb{R}^2$  (non-unique):

$$\nabla\Phi(\llbracket u_{hn} \rrbracket, \lambda_h) = (\mathbf{1}_{\mathcal{A}(\llbracket u_{hn} \rrbracket, \lambda_h)}, -r\mathbf{1}_{\mathcal{I}(\llbracket u_{hn} \rrbracket, \lambda_h)}), \tag{4.3}$$

with the indicator function  $\mathbf{1}_{\{\cdot\}}$  of the strictly active set:

$$\mathcal{A}(\llbracket u_{hn} \rrbracket, \lambda_h) = \{\mathbf{x} \in \Gamma_C^h \mid (\llbracket u_{hn} \rrbracket + r\lambda_h)(\mathbf{x}) < 0\}, \tag{4.4}$$

and its complementary inactive set of nodes:

$$\mathcal{I}(\llbracket u_{hn} \rrbracket, \lambda_h) = \{\mathbf{x} \in \Gamma_C^h \mid (\llbracket u_{hn} \rrbracket + r\lambda_h)(\mathbf{x}) \geq 0\}. \tag{4.5}$$

The function  $\Phi(y)$  is semi-smooth in the following sense of asymptotic estimate:

$$\begin{cases} \|\delta\Phi\|_\infty = o(\|\delta y\|_\infty) \quad \text{as } \delta y := \llbracket u_{hn} - v_{hn} \rrbracket + r(\lambda_h - \mu_h) \rightarrow 0, \\ \text{where } \delta\Phi := \Phi(\llbracket u_{hn} \rrbracket, \lambda_h) - \Phi(\llbracket v_{hn} \rrbracket, \mu_h) - \nabla\Phi(\llbracket u_{hn} \rrbracket, \lambda_h) \cdot (\llbracket u_{hn} - v_{hn} \rrbracket, \lambda_h - \mu_h), \end{cases} \tag{4.6}$$

using the supremum norm  $\|\cdot\|_\infty$  and Landau “little-o” notation.

**Proof.** Using the active (4.4) and the inactive (4.5) sets we reformulate (4.1) as

$$\Phi(\llbracket u_{hn} \rrbracket, \lambda_h) = \llbracket u_{hn} \rrbracket \mathbf{1}_{\mathcal{A}(\llbracket u_{hn} \rrbracket, \lambda_h)} - r \lambda_h \mathbf{1}_{\mathcal{I}(\llbracket u_{hn} \rrbracket, \lambda_h)}. \tag{4.7}$$

From (4.3) and (4.7) it can be calculated the function increment:

$$\delta\Phi = \llbracket v_{hn} \rrbracket (\mathbf{1}_{\mathcal{A}(\llbracket u_{hn} \rrbracket, \lambda_h)} - \mathbf{1}_{\mathcal{A}(\llbracket v_{hn} \rrbracket, \mu_h)}) - r \mu_h (\mathbf{1}_{\mathcal{I}(\llbracket u_{hn} \rrbracket, \lambda_h)} - \mathbf{1}_{\mathcal{I}(\llbracket v_{hn} \rrbracket, \mu_h)}).$$

For  $(\llbracket u_{hn} \rrbracket, \lambda_h)$  fixed,  $\delta\Phi = 0$  for all argument increments  $\delta y$  which are small:

$$\|\delta y\|_\infty < \min\{\mathbf{x} \in \Gamma_C^h \mid (\llbracket u_{hn} \rrbracket + r \lambda_h)(\mathbf{x}) \neq 0\}.$$

In particular, this implies the asymptotic estimate (4.6).  $\square$

**Remark 4.1.** Geometrically, (4.6) defines a slant asymptote, which is the consequence of smooth derivative if it exists.

**Remark 4.2.** For the proof of Lemma 4.1 for  $\Phi : L^p(\Gamma_C)^2 \mapsto L^2(\Gamma_C)$  with  $p > 2$  see [29] and references therein.

**Remark 4.3.** In (4.1) the nonlinear equation  $\Phi(\llbracket u_{hn}^{m+\alpha} \rrbracket, \lambda_h^{m+\alpha}) = 0$  can be rewritten in the classical form:

$$\lambda_h^{m+\alpha} = \frac{1}{r} \min(\llbracket u_{hn}^{m+\alpha} \rrbracket + r \lambda_h^{m+\alpha}, 0).$$

Decomposing  $\llbracket v_{hn} \rrbracket = \llbracket v_{hn} \rrbracket + r \mu_h - r \mu_h$  and inserting it into (4.2) as

$$\begin{cases} \mathbf{A}_\tau(\mathbf{u}_h^{m+\alpha}, \mathbf{v}_h) + \frac{1}{r} \min(\llbracket u_{hn}^{m+\alpha} \rrbracket + r \lambda_h^{m+\alpha}, 0) \cdot (\llbracket v_{hn} \rrbracket + r \mu_h) - r \lambda_h^{m+\alpha} \cdot \mu_h \\ = \mathbf{F}_\tau^m(\mathbf{v}_h) \quad \text{for all } (\mathbf{v}_h, \mu_h) \in \mathbf{V}_h \times \mathbb{R}^{N_C^h} \end{cases} \tag{4.8}$$

was useful to formulate the Nitsche method in [20,21].

Based on the generalized gradient  $\nabla\Phi$  from Lemma 4.1 we formulate the Newton method for solution of the nonlinear system of Eqs. (4.2). Initialize with some guess  $(\mathbf{u}_h^{m+\alpha,0}, \lambda_h^{m+\alpha,0}) \in \mathbf{V}_h \times \mathbb{R}^{N_C^h}$  at  $k = 0$ , at every integer  $k \geq 0$  solve

$$\begin{cases} \mathbf{A}_\tau(\mathbf{u}_h^{m+\alpha,k+1} - \mathbf{u}_h^{m+\alpha,k}, \mathbf{v}_h) + (\lambda_h^{m+\alpha,k+1} - \lambda_h^{m+\alpha,k}) \llbracket v_{hn} \rrbracket \\ = \mathbf{F}_\tau^m(\mathbf{v}_h) - \mathbf{A}_\tau(\mathbf{u}_h^{m+\alpha,k}, \mathbf{v}_h) - \lambda_h^{m+\alpha,k} \cdot \llbracket v_{hn} \rrbracket \quad \text{for all } \mathbf{v}_h \in \mathbf{V}_h, \\ \nabla\Phi(\llbracket u_{hn}^{m+\alpha,k} \rrbracket, \lambda_h^{m+\alpha,k}) \cdot (\llbracket u_{hn}^{m+\alpha,k+1} - u_{hn}^{m+\alpha,k} \rrbracket, \lambda_h^{m+\alpha,k+1} - \lambda_h^{m+\alpha,k}) \\ = -\Phi(\llbracket u_{hn}^{m+\alpha,k} \rrbracket, \lambda_h^{m+\alpha,k}), \end{cases}$$

which after the insertion of (4.3) and (4.7) yields the following linear system:

$$\begin{cases} \text{Find } (\mathbf{u}_h^{m+\alpha,k+1}, \lambda_h^{m+\alpha,k+1}) \in \mathbf{V}_h \times \mathbb{R}^{N_C^h} \text{ such that:} \\ \mathbf{A}_\tau(\mathbf{u}_h^{m+\alpha,k+1}, \mathbf{v}_h) + \lambda_h^{m+\alpha,k+1} \cdot \llbracket v_{hn} \rrbracket = \mathbf{F}_\tau^m(\mathbf{v}_h) \quad \text{for all } \mathbf{v}_h \in \mathbf{V}_h, \\ \llbracket u_{hn}^{m+\alpha,k+1} \rrbracket \mathbf{1}_{\mathcal{A}(\llbracket u_{hn}^{m+\alpha,k} \rrbracket, \lambda_h^{m+\alpha,k})} - r \lambda_h^{m+\alpha,k+1} \mathbf{1}_{\mathcal{I}(\llbracket u_{hn}^{m+\alpha,k} \rrbracket, \lambda_h^{m+\alpha,k})} = 0. \end{cases} \tag{4.9}$$

Following [29], we state the well-posedness and local convergence result.

**Theorem 4.1.** *At each  $k$ , the semi-smooth Newton iterate (4.9) admits one unique solution. If the initial guess is chosen sufficiently close to the solution, then the sequence of iterates converges super-linearly with the estimate:*

$$\begin{cases} \|\mathbf{u}_h^{m+\alpha,k+1} - \mathbf{u}_h^{m+\alpha,k}\|_{1,\Omega} + \|\lambda_h^{m+\alpha,k+1} - \lambda_h^{m+\alpha,k}\|_\infty = o(\|\delta y^k\|_\infty) \\ \text{as } \delta y^k := \llbracket u_{hn}^{m+\alpha,k} - u_{hn}^{m+\alpha} \rrbracket + r(\lambda_h^{m+\alpha,k} - \lambda_h^{m+\alpha}) \rightarrow 0. \end{cases} \tag{4.10}$$

**Proof.** Owing to  $\lambda_h^{m+\alpha,k+1} = 0$  on the inactive set  $\mathcal{I}(\llbracket u_{hn}^{m+\alpha,k} \rrbracket, \lambda_h^{m+\alpha,k})$ , system (4.9) can be expressed as the Dirichlet problem on the active set:

$$\begin{cases} \text{Find } \mathbf{u}_h^{m+\alpha,k+1} \in \mathbf{V}_h \text{ such that:} \\ \llbracket u_{hn}^{m+\alpha,k+1} \rrbracket = 0 \quad \text{on } \mathcal{A}(\llbracket u_{hn}^{m+\alpha,k} \rrbracket, \lambda_h^{m+\alpha,k}), \\ \mathbf{A}_\tau(\mathbf{u}_h^{m+\alpha,k+1}, \mathbf{v}_h) = \mathbf{F}_\tau^m(\mathbf{v}_h) \\ \text{for all } \mathbf{v}_h \in \mathbf{V}_h \text{ with } \llbracket v_{hn} \rrbracket = 0 \text{ on } \mathcal{A}(\llbracket u_{hn}^{m+\alpha,k} \rrbracket, \lambda_h^{m+\alpha,k}). \end{cases}$$

The bounded and coercive operator  $\mathbf{A}_\tau$  (see (3.13)) is one-to-one, thus justifying well-posedness to the Newton iterate.

Using the identity  $\Phi(\llbracket u_{hn} \rrbracket + r \lambda_h, 0) = (\llbracket u_{hn} \rrbracket + r \lambda_h) \mathbf{1}_{\mathcal{A}(\llbracket u_{hn} \rrbracket, \lambda_h)}$  and the notation of increment  $\delta y^k$  in (4.10), we assemble the terms

as follows:

$$r\lambda_h^{m+\alpha,k+1} = (\llbracket u_{hn}^{m+\alpha,k+1} \rrbracket + r\lambda_h^{m+\alpha,k}) \mathbf{1}_{\mathcal{A}(\llbracket u_{hn}^{m+\alpha,k} \rrbracket, \lambda_h^{m+\alpha,k})}$$

$$= \Phi(\llbracket u_{hn}^{m+\alpha,k} \rrbracket + r\lambda_h^{m+\alpha,k}, 0) + \delta y^{k+1} - \delta y^k.$$

Subtract here  $r\lambda_h^{m+\alpha} = \Phi(\llbracket u_{hn}^{m+\alpha} \rrbracket + r\lambda_h^{m+\alpha}, 0)$  according to (4.9), which yields

$$\begin{cases} \llbracket u_{hn}^{m+\alpha,k} - u_{hn}^{m+\alpha} \rrbracket \mathbf{1}_{\mathcal{A}(\llbracket u_{hn}^{m+\alpha,k} \rrbracket, \lambda_h^{m+\alpha,k})} - r(\lambda_h^{m+\alpha,k} - \lambda_h^{m+\alpha}) \mathbf{1}_{\mathcal{I}(\llbracket u_{hn}^{m+\alpha,k} \rrbracket, \lambda_h^{m+\alpha,k})} \\ = -\delta\Phi^k, \end{cases} \tag{4.11}$$

where  $\delta\Phi^k := \Phi(\llbracket u_{hn}^{m+\alpha,k} \rrbracket + r\lambda_h^{m+\alpha,k}, 0) - \Phi(\llbracket u_{hn}^{m+\alpha} \rrbracket + r\lambda_h^{m+\alpha}, 0) - \Phi'(\llbracket u_{hn}^{m+\alpha,k} \rrbracket + r\lambda_h^{m+\alpha,k}, 0)\delta y^k,$

and thanks to (4.6) the asymptotic estimate takes place:

$$\|\delta\Phi^k\|_\infty = o(\|\delta y^k\|_\infty) \text{ as } \delta y^k \rightarrow 0. \tag{4.12}$$

From the difference of problems (4.2) and (4.9) we infer the equation:

$$\begin{cases} \mathbf{A}_\tau(\mathbf{u}_h^{m+\alpha,k+1} - \mathbf{u}_h^{m+\alpha}, \mathbf{v}_h) = -(\lambda_h^{m+\alpha,k+1} - \lambda_h^{m+\alpha}) \cdot \llbracket u_{hn} \rrbracket \\ \text{for all } \mathbf{v}_h \in \mathbf{V}_h. \end{cases} \tag{4.13}$$

For any  $\phi \in \mathbb{R}^{N_C^h}$  let us consider extensions  $\mathbf{v}_h \in \mathbf{V}_h$  such that  $\llbracket u_{hn} \rrbracket = \phi$  on  $\Gamma_C^h$  which are bounded:  $\|\mathbf{v}_h\|_{1,\Omega} \leq C\|\llbracket u_{hn} \rrbracket\|_\infty$  with constant  $C > 0$ . Then using the upper bound (3.5) we estimate from (4.13) the dual norm:

$$\|\lambda_h^{m+\alpha,k+1} - \lambda_h^{m+\alpha}\|_\infty = \sup_{\phi \in \mathbb{R}^{N_C^h}} \frac{|(\lambda_h^{m+\alpha,k+1} - \lambda_h^{m+\alpha}) \cdot \phi|}{\|\phi\|_\infty}$$

$$\leq \left(\frac{\rho}{\alpha\beta\tau^2} + C_E\right) C \|\mathbf{u}_h^{m+\alpha,k+1} - \mathbf{u}_h^{m+\alpha}\|_{1,\Omega}. \tag{4.14}$$

On the other side, testing (4.13) with  $\mathbf{v}_h = \mathbf{u}_h^{m+\alpha,k+1} - \mathbf{u}_h^{m+\alpha}$ , applying the lower bound (3.13) and (4.11) it follows that

$$\left(\frac{\rho h^2}{\alpha\beta\tau^2} C_1^2 + C_K\right) \|\mathbf{u}_h^{m+\alpha,k+1} - \mathbf{u}_h^{m+\alpha}\|_{1,\Omega}^2 \leq \|\delta\Phi^k\|_\infty \left(\|\frac{1}{r}\llbracket u_{hn}^{m+\alpha,k} - u_{hn}^{m+\alpha} \rrbracket\|_\infty + \|\lambda_h^{m+\alpha,k} - \lambda_h^{m+\alpha}\|_\infty\right).$$

The inequalities (4.14) and (4.15) in the virtue of (4.12) provide the asymptotic estimate (4.10). For the initial guess  $(\mathbf{u}_h^{m+\alpha,0}, \lambda_h^{m+\alpha,0})$  chosen sufficiently close to the solution  $(\mathbf{u}_h^{m+\alpha}, \lambda_h^{m+\alpha})$  of the problem (4.2), this estimate validates the super-linear convergence of the semi-smooth Newton iterates as  $m \rightarrow \infty$ .  $\square$

Next we propose a globalization procedure for arbitrary initialization.

#### 4.1. Primal–dual active set (PDAS) algorithm

For analysis of the Newton iterate (4.9) represented equivalently as

$$\begin{cases} \text{Find } (\mathbf{u}_h^{m+\alpha,k+1}, \lambda_h^{m+\alpha,k+1}) \in \mathbf{V}_h \times \mathbb{R}^{N_C^h} \text{ such that:} \\ \mathbf{A}_\tau(\mathbf{u}_h^{m+\alpha,k+1}, \mathbf{v}_h) + \lambda_h^{m+\alpha,k+1} \cdot \llbracket u_{hn} \rrbracket = \mathbf{F}_\tau(\mathbf{v}_h) \text{ for all } \mathbf{v}_h \in \mathbf{V}_h, \\ \llbracket u_{hn}^{m+\alpha,k+1} \rrbracket = 0 \text{ on } \mathcal{A}(\llbracket u_{hn}^{m+\alpha,k} \rrbracket, \lambda_h^{m+\alpha,k}), \\ \lambda_h^{m+\alpha,k+1} = 0 \text{ on } \mathcal{I}(\llbracket u_{hn}^{m+\alpha,k} \rrbracket, \lambda_h^{m+\alpha,k}), \end{cases} \tag{4.15}$$

we write (4.15) in the algebraic form using mass and stiffness matrices. Applying the Schur complement reduces the matrix equation to the system with respect to the constrained components  $\mathbf{U}^k = \llbracket u_{hn}^{m+\alpha,k} \rrbracket$  and  $\mathbf{A}^k = \lambda_h^{m+\alpha,k}$ :

$$\begin{cases} \mathbf{M}\mathbf{U}^{k+1} + \mathbf{A}^{k+1} = \mathbf{F}, \\ \mathbf{U}^{k+1} = 0 \text{ on } \mathcal{A}(\mathbf{U}^k, \mathbf{A}^k) = \mathcal{A}^k, \\ \mathbf{A}^{k+1} = 0 \text{ on } \mathcal{I}(\mathbf{U}^k, \mathbf{A}^k) = \mathcal{I}^k, \end{cases} \tag{4.16}$$

where the system matrix  $\mathbf{M} \in \mathbb{R}^{N_C^h \times N_C^h}$  and the right-hand side  $\mathbf{F} \in \mathbb{R}^{N_C^h}$ .

#### Algorithm 4.1 (PDAS algorithm).

**Initialization:** Choose  $\mathcal{A}^{-1} \subset \{1, \dots, N_C^h\}$  and its complementary set  $\mathcal{I}^{-1}$ , set iteration number  $k = -1$ .

**Iteration step:** Solve for  $(\mathbf{U}^{k+1}, \mathbf{A}^{k+1}) \in \mathbb{R}^{N_C^h} \times \mathbb{R}^{N_C^h}$  the linear system (4.16). Compute the active and inactive sets of indexes:

$$\begin{cases} \mathcal{A}^{k+1} = \{i \in \{1, \dots, N_C^h\} \mid (\mathbf{U}^{k+1} + r\mathbf{A}^{k+1})_i < 0\}, \\ \mathcal{I}^{k+1} = \{i \in \{1, \dots, N_C^h\} \mid (\mathbf{U}^{k+1} + r\mathbf{A}^{k+1})_i \geq 0\}. \end{cases} \tag{4.17}$$

**Stopping rule:** If  $\mathcal{A}^{k+1} = \mathcal{A}^k$  then stop with the exact solution  $(\mathbf{U}, \mathbf{\Lambda}) = (\mathbf{U}^{k+1}, \mathbf{\Lambda}^{k+1})$  of the linear complementarity problem (LCP):

$$\begin{cases} \mathbf{M}\mathbf{U} + \mathbf{\Lambda} = \mathbf{F}, \\ \mathbf{U} = 0 \quad \text{on } \mathcal{A}(\mathbf{U}, \mathbf{\Lambda}), \\ \mathbf{\Lambda} = 0 \quad \text{on } \mathcal{I}(\mathbf{U}, \mathbf{\Lambda}), \end{cases} \tag{4.18}$$

else iterate the solution of (4.16) at the iteration step  $k = k + 1$ .

The solution of LCP (4.18) implies the constrained components  $\mathbf{U} = \llbracket u_{hh}^{m+\alpha} \rrbracket$  and  $\mathbf{\Lambda} = \lambda_h^{m+\alpha}$  of the primal–dual variational problem (3.11). Following [29], we recall the result on monotone global convergence.

**Proposition 4.1.** *Let the system matrix  $\mathbf{M} = (M_{ij})$  be M-matrix:*

$$\begin{cases} M_{ii} > 0, \quad M_{ij} \leq 0 \text{ for } j \neq i, \\ \text{there exists the positive inverse matrix } \mathbf{M}^{-1} \geq 0. \end{cases} \tag{4.19}$$

If the  $k$ th iterate of Algorithm 4.1 is feasible:  $\mathbf{U}^k \geq 0$ , then all subsequent iterates are feasible and monotone together with the active sets such that:

$$\begin{cases} 0 \leq \mathbf{U}^k \leq \mathbf{U}^{k+1} \leq \dots \leq \mathbf{U}, \\ \mathcal{A}^k \supseteq \mathcal{A}^{k+1} \supseteq \dots \supseteq \mathcal{A}(\mathbf{U}, \mathbf{\Lambda}). \end{cases} \tag{4.20}$$

For the initial guess  $\mathcal{A}^{-1} = \emptyset$  the 1st iterate is feasible. When reaching a feasible iterate, exact solution to the LCP (4.18) is attained in a finite number of steps.

**Proof.** Let us split the matrix equation in (4.16) into the blocks:

$$\begin{cases} \mathbf{M}_{\mathcal{A}^k \mathcal{A}^k} \mathbf{U}_{\mathcal{A}^k}^{k+1} + \mathbf{M}_{\mathcal{A}^k \mathcal{I}^k} \mathbf{U}_{\mathcal{I}^k}^{k+1} + \mathbf{\Lambda}_{\mathcal{A}^k}^{k+1} = \mathbf{F}_{\mathcal{A}^k}, \\ \mathbf{M}_{\mathcal{I}^k \mathcal{A}^k} \mathbf{U}_{\mathcal{A}^k}^{k+1} + \mathbf{M}_{\mathcal{I}^k \mathcal{I}^k} \mathbf{U}_{\mathcal{I}^k}^{k+1} + \mathbf{\Lambda}_{\mathcal{I}^k}^{k+1} = \mathbf{F}_{\mathcal{I}^k}, \end{cases} \tag{4.21}$$

where  $\mathbf{U}_{\mathcal{A}^k}^{k+1} = 0$  and  $\mathbf{\Lambda}_{\mathcal{I}^k}^{k+1} = 0$ , and similarly at the  $k$ th iterate:

$$\begin{cases} \mathbf{M}_{\mathcal{A}^k \mathcal{A}^k} \mathbf{U}_{\mathcal{A}^k}^k + \mathbf{M}_{\mathcal{A}^k \mathcal{I}^k} \mathbf{U}_{\mathcal{I}^k}^k + \mathbf{\Lambda}_{\mathcal{A}^k}^k = \mathbf{F}_{\mathcal{A}^k}, \\ \mathbf{M}_{\mathcal{I}^k \mathcal{A}^k} \mathbf{U}_{\mathcal{A}^k}^k + \mathbf{M}_{\mathcal{I}^k \mathcal{I}^k} \mathbf{U}_{\mathcal{I}^k}^k + \mathbf{\Lambda}_{\mathcal{I}^k}^k = \mathbf{F}_{\mathcal{I}^k}. \end{cases} \tag{4.22}$$

Within the iteration either  $U_i^k = 0$  or  $\Lambda_i^k = 0$  for all  $i$ , such that  $U_i^k \leq 0, \Lambda_i^k \leq 0$  for  $i \in \mathcal{A}^k$ , and  $U_i^k \geq 0, \Lambda_i^k \geq 0$  for  $i \in \mathcal{I}^k$  in (4.17). Therefore,

$$\mathbf{U}_{\mathcal{A}^k}^{k+1} - \mathbf{U}_{\mathcal{A}^k}^k = -\mathbf{U}_{\mathcal{A}^k}^k \geq 0, \quad \mathbf{\Lambda}_{\mathcal{I}^k}^{k+1} - \mathbf{\Lambda}_{\mathcal{I}^k}^k = -\mathbf{\Lambda}_{\mathcal{I}^k}^k \leq 0.$$

Calculating the difference between (4.21) and (4.22) it follows

$$\mathbf{U}_{\mathcal{I}^k}^{k+1} - \mathbf{U}_{\mathcal{I}^k}^k = -\mathbf{M}_{\mathcal{I}^k \mathcal{I}^k}^{-1} \mathbf{M}_{\mathcal{I}^k \mathcal{A}^k} (\mathbf{U}_{\mathcal{A}^k}^{k+1} - \mathbf{U}_{\mathcal{A}^k}^k) - \mathbf{M}_{\mathcal{I}^k \mathcal{I}^k}^{-1} (\mathbf{\Lambda}_{\mathcal{I}^k}^{k+1} - \mathbf{\Lambda}_{\mathcal{I}^k}^k) \geq 0, \tag{4.23}$$

since  $\mathbf{M}_{\mathcal{I}^k \mathcal{I}^k}^{-1} \geq 0$  and  $\mathbf{M}_{\mathcal{I}^k \mathcal{A}^k} \leq 0$  as a consequence of the assumption (4.19). When starting with feasible  $\mathbf{U}^k \geq 0$  we conclude with feasible  $\mathbf{U}^{k+1} \geq 0$  and the monotony  $\mathbf{U}^{k+1} - \mathbf{U}^k \geq 0$  of all subsequent iterates.

From the feasibility of  $\mathbf{U}^{k+1}$  and  $\mathbf{\Lambda}_{\mathcal{I}^k}^{k+1} = 0$  we derive that  $U_i^{k+1} + r\Lambda_i^{k+1} \geq 0$  for  $i \in \mathcal{I}^k$ , hence  $\mathcal{I}^{k+1} \supseteq \mathcal{I}^k$ , which justifies the monotone properties in (4.20).

For the initialization  $\mathcal{A}^{-1} = \emptyset$  we have  $\mathbf{\Lambda}^0 = \mathbf{0}$  implying that  $\mathbf{U}_{\mathcal{I}^0}^0 \geq 0$ . Then  $\mathbf{U}_{\mathcal{I}^0}^1 \geq \mathbf{U}_{\mathcal{I}^0}^0$  owing to (4.23) and  $\mathbf{U}_{\mathcal{A}^0}^1 = 0$  provide feasibility for the 1st iterate.

The monotony of active and inactive sets in finite dimensions guarantees that the stopping rule in Algorithm 4.1 is attained after a finite number of iterations. If  $\mathcal{A}^{k+1} = \mathcal{A}^k$ , then from (4.16) and (4.17) it follows that the iterate  $\mathbf{U}^{k+1} \geq 0$  on  $\mathcal{I}^{k+1}$  and  $\mathbf{\Lambda}^{k+1} < 0$  on  $\mathcal{A}^{k+1}$ , hence fulfills the complementarity conditions:

$$\mathbf{U}_i^{k+1} \geq 0, \quad \mathbf{\Lambda}_i^{k+1} \leq 0, \quad \mathbf{\Lambda}_i^{k+1} \mathbf{U}_i^{k+1} = 0 \quad \text{for } i \in \{1, \dots, N_C^h\}$$

implying (4.18). The proof is complete.  $\square$

**Remark 4.4.** Consider Example 2.1. It is known that the standard  $\mathbb{P}_1$ -FEM on uniform grids builds a stiffness matrix for Laplacian which has M-property. According to [29] a small perturbation of M-matrix and its Schur complement is an M-matrix again. This justifies the assumption (4.19) in Proposition 4.1.

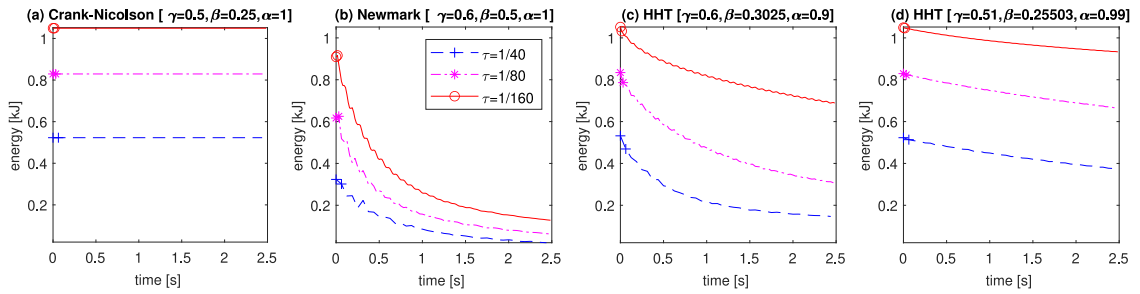


Fig. 2. The compression-release benchmark: discrete energy  $E_h^m$  versus time  $t^m$  for the selected in plots (a)–(d) parameters  $[\gamma, \beta, \alpha]$  when decreasing the time step  $\tau$ .

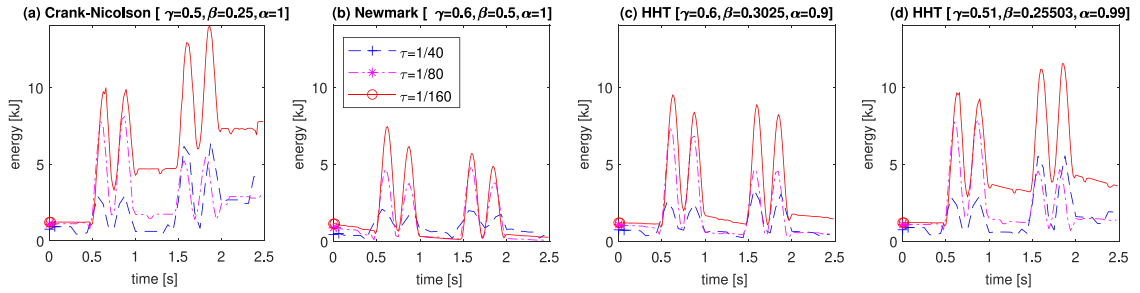


Fig. 3. The double impact benchmark: discrete energy  $E_h^m$  versus time  $t^m$  for the selected in plots (a)–(d) parameters  $[\gamma, \beta, \alpha]$  when decreasing the time step  $\tau = 1/160, 1/80, 1/40$ .

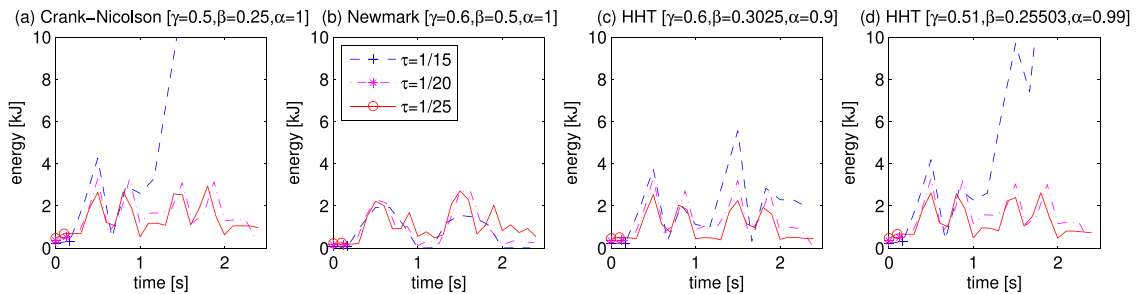


Fig. 4. The double impact benchmark: discrete energy  $E_h^m$  versus time  $t^m$  for the selected in plots (a)–(d) parameters  $[\gamma, \beta, \alpha]$  when decreasing the time step  $\tau = 1/25, 1/20, 1/15$ .

5. Numerical example of dynamic signorini contact

In what follows we consider a Signorini contact problem. Let the 1st-body be rigid such that  $\mathbf{u}^1 = \mathbf{0}$  and  $\mathbf{u}^2 = \mathbf{u}$ .

We utilize the standard piecewise linear  $\mathbb{P}_1$ -polynomial approximation in the FEM space  $\mathbf{V}_h^2$ . After the full discretization, the dynamic Signorini contact problem (3.9) reads in the body  $\Omega^2$ :

$$\begin{cases} \text{Find } (\mathbf{u}_h^{m+\alpha}, \lambda_h^{m+\alpha}) \in \mathbf{V}_h^2 \times \mathbb{R}^{N_C^h} \text{ such that:} \\ \mathbf{A}_\tau(\mathbf{u}_h^{m+\alpha}, \mathbf{v}_h) + \lambda_h^{m+\alpha} \cdot (\psi - v_{hn}) = \mathbf{F}_\tau^m(\mathbf{v}_h) \text{ for all } \mathbf{v}_h \in \mathbf{V}_h^2, \\ u_{hn}^{m+\alpha} \leq \psi, \quad \lambda_h^{m+\alpha} \leq 0, \quad \lambda_h^{m+\alpha}(\psi - u_{hn}^{m+\alpha}) = 0 \text{ on } \Gamma_C^h, \end{cases} \tag{5.1}$$

where  $\psi = (\mathbf{u}^1 \circ \Pi^1) \cdot \mathbf{n}$  from (2.8). For simulation we choose the 2D-geometry:

$$\begin{cases} \Omega^2 = \{\mathbf{x} \in (0, L_1) \times (0, L_2)\}, \quad L_1 = 2.5 \text{ [m]}, \quad L_2 = 1 \text{ [m]}, \\ \Gamma_D^2 = \{x_2 = 0\}, \quad \Gamma_N^2 = \{x_1 = 0, L_1\}, \quad \Gamma_C = \{x_2 = L_2\}, \end{cases}$$

with contact surface  $\Gamma_C = \Gamma_C^1 = \Gamma_C^2$  and  $\psi = 0$ . The parameters of isotropic body are: density  $\rho = 2700$  [kg/m<sup>3</sup>], Young’s modulus  $E = 73000$  [mPa] and Poisson ratio  $\nu = 0.34$  entering Lamé parameters  $\lambda_L = 2\mu_L\nu/(1 - 2\nu)$  and  $\mu_L = E/(2(1 + \nu))$ .

To examine stability we propose benchmark in which the body is compressed with the uniform body force  $f_2 = 50$  [kN] at  $t^0 = 0$ , then released with  $\dot{\mathbf{u}}_h^0 = \mathbf{0}$  and  $\ddot{\mathbf{u}}_h^0 = \mathbf{0}$  for  $t^m \in (0, 2.5)$  [s]. In Fig. 2 there is depicted the discrete energy from formula (3.15). The

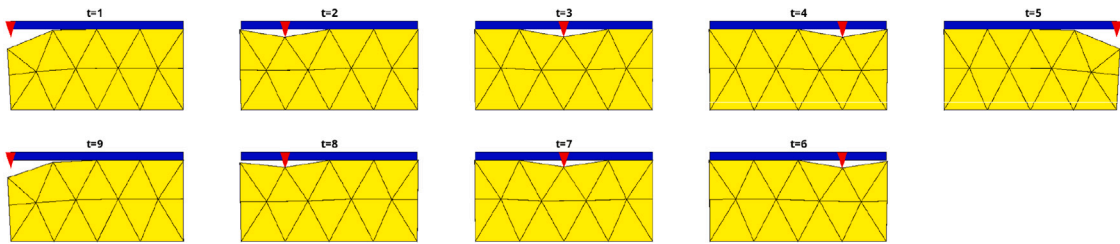


Fig. 5. Displacement under moving vertical load in the current configuration  $x + u_h^m$ .

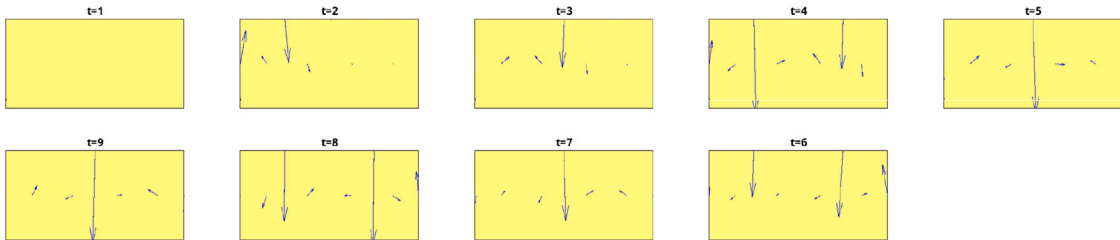


Fig. 6. Vectors of velocity  $\dot{u}_h^m$  at nodes of the body under moving vertical load.

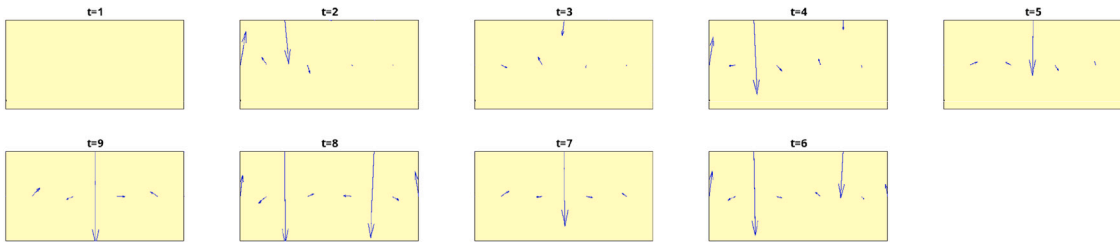


Fig. 7. Vectors of acceleration  $\ddot{u}_h^m$  at nodes of the body under moving vertical load.

solution  $u_h^m, \dot{u}_h^m$  is computed by the HHT- $\alpha$  scheme (3.4) for the fixed mesh size  $h = 1/20$  and time step  $\tau = 1/160, 1/80, 1/40$ , so the Courant number varies  $v_C := \tau v_c / h \in \{v_c/8, v_c/4, v_c/2\}$ , with  $v_c = \sqrt{E/\rho} \approx 5200$  [m/s] the speed of compression waves. In Fig. 2 we compare the standard Crank–Nicolson (CN) scheme [ $\gamma = 0.5, \beta = 0.25$ ] (left) with the  $\gamma$ -damped Newmark scheme [ $\gamma = 0.6, \beta = 0.5$ ] (center-left) from [37] as  $\alpha = 1$ , and two  $\alpha$ -damped schemes for [ $\gamma = 0.6, \beta = 0.3025, \alpha = 0.9$ ] (center-right) from [35,37] and [ $\gamma = 0.51, \beta = 0.255025, \alpha = 0.99$ ] (right). Within the release phase, the energy is constant in the plot (a) because CN is energy preserving in the purely elastic case, and the energy does not increase in time in all other plots (b)–(d).

The second benchmark is associated with a double impact in the structure presented in the experiment by [16]. The initially compressed body is released as before, first compressed with the uniform body force  $f_2$  for  $t^m \in (0.5, 1]$  [s] then released, and gets compressed second time for  $t^m \in (1.5, 2]$  [s] then released again. For the discretization parameters as before, the spurious oscillations in the energy are suppressed by the implicit Newmark scheme in the plot (b) and by the HHT- $\alpha$  schemes in plots (c) and (d) of Fig. 3. From benchmark it is clear that Crank–Nicolson is unstable, Newmark  $\gamma = 0.6$  is too much dissipative, and HHT  $\alpha = 0.99$  is not sufficiently dissipative. Fig. 4 depicts FEM solution for the Courant number fixed at  $v_C = 2v_c$  implying that both mesh and step sizes vary simultaneously when  $\tau = 1/25, 1/20, 1/15$ . The discrete energy is convergent within this simulation time.

For the choice of weight  $\alpha$  we remark the following. Increasing the parameter  $\alpha > 1$  (that is  $\bar{\alpha} < 0$  in [36]) reduces the mass matrix in (3.10), hence M-property of the system matrix  $M$  that is assumed in Proposition 4.1 may be lost. As the consequence, loss of the monotone property of Newton iterates may cause cycling of the algorithm and lead to numerical instabilities of the solution.

The other difficulty concerns the so-called grazing contact when the bodies only touch each other, that is both  $\|u_{hn}^{m+\alpha}\|$  and  $\lambda_h^{m+\alpha}$  are almost zeros, thus posed on the boundary between active and inactive sets. To remedy numerical instabilities in this case we suggest to use a small gap  $\delta > 0$  such that  $\|u_{hn}\| + r\lambda_h < \delta$  in (4.4), respectively  $\|u_{hn}\| + r\lambda_h \geq \delta$  in (4.5). In our simulation we have used  $\delta = 10^{-5}$ .

### 5.1. Elastodynamic response to a moving load

Now boundary load at the contact surface is summed from reaction to the gravitational mass  $m^1$  of the 1st body and moving vertical load prescribed by the hat-function  $\delta_h(x_1 - t)$  in a small  $h$ -neighborhood of  $x_1 = t$  such that the body force for the forward

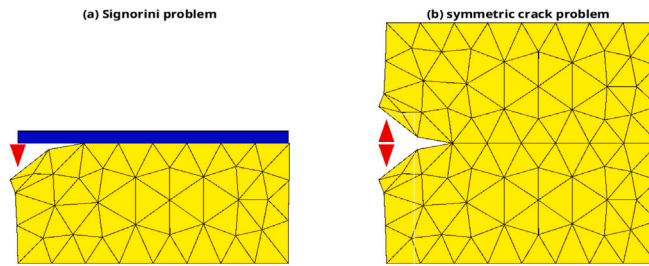


Fig. 8. The standard Crank–Nicolson scheme: maximal amplitude of horizontal displacements  $u_{h1}$  (a) and vertical displacements  $u_{h2}$  (b) within two consequent motion loops.

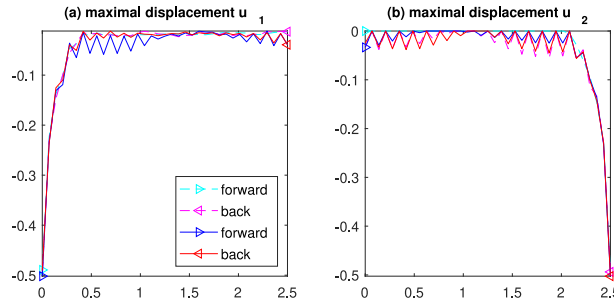


Fig. 9. The HHT [ $\gamma = 0.6, \beta = 0.3025, \alpha = 0.98$ ]: maximal amplitude of horizontal displacements  $u_{h1}$  (a) and vertical displacements  $u_{h2}$  (b) within two consequent motion loops.

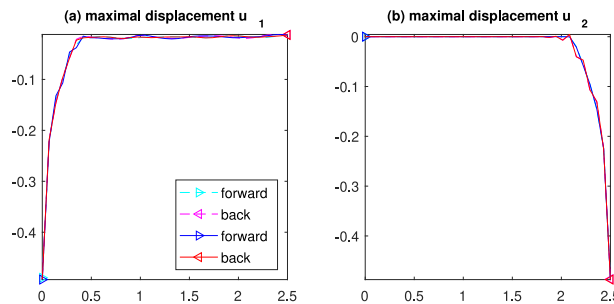


Fig. 10. Iterates  $k$  of the PDAS algorithm: the contact opening  $U^k$  (a); Lagrange multiplier  $A^k$  (b); active set  $\mathcal{A}^k$  (c).

motion for  $t \in [0, L_1]$ :

$$\int_{\Omega^2} \mathbf{f}(t) \cdot \mathbf{v}_h \, d\mathbf{x} = \int_{\Omega^2} (0, m^1 g) \cdot \mathbf{v}_h \, d\mathbf{x} - \int_{\Gamma_C} (0, \mu_L \delta_h(t)) \cdot \mathbf{v}_h \, d\Gamma, \tag{5.2}$$

and for the backward motion for  $t \in (L_1, 2L_1]$ :

$$\int_{\Omega^2} \mathbf{f}(t) \cdot \mathbf{v}_h \, d\mathbf{x} = \int_{\Omega^2} (0, m^1 g) \cdot \mathbf{v}_h \, d\mathbf{x} - \int_{\Gamma_C} (0, \mu_L \delta_h(2L_1 - t)) \cdot \mathbf{v}_h \, d\Gamma, \tag{5.3}$$

where  $m^1 = 5 \times 10^3$  [kg] and  $g = 9.81$  [m/s<sup>2</sup>]. For illustration reason, we present the motion loop at time steps  $m = 1, \dots, 9$  of initially compressed body in the current configuration  $\mathbf{x} + \mathbf{u}_h^m$  (where  $h = 0.5$ ) for  $\mathbf{x} \in \Omega^2$  in Fig. 5. The corresponding vectors of velocity  $\dot{\mathbf{u}}_h^m$  are depicted at nodal points in Fig. 6, and acceleration  $\ddot{\mathbf{u}}_h^m$  in Fig. 7 within quiver plots over  $\Omega^2$ .

It is worth noting that the computed solution describes also the solution

$$\begin{cases} u_{h1}^{1m}(\mathbf{x}) = u_{h1}^{2m}(x_1, 2L_2 - x_2), & u_{h2}^{1m}(\mathbf{x}) = -u_{h2}^{2m}(x_1, 2L_2 - x_2) \quad \text{for } \mathbf{x} \in \Omega^1, \\ \Omega^1 = \{\mathbf{x} \in (0, L_1) \times (L_2, 2L_2)\}, & \Gamma_D^1 = \{x_2 = 2L_2\}, & \Gamma_N^1 = \{x_1 = 0, L_1\}, \end{cases}$$

to a symmetric problem with crack depicted in Fig. 11 in the current configuration  $\mathbf{x} + \mathbf{u}_h^0$  at  $m = 0$  in  $\Omega^1 \cup \Omega^2$ . Due to the mirror symmetry of the problem, the transmission conditions hold on the active set of  $\Gamma_C^h$ :

$$\llbracket u_{h1}^0 \rrbracket = 0, \quad \llbracket u_{h2}^0 \rrbracket = 0, \quad \llbracket \sigma_{12}(\mathbf{u}_h^0) \rrbracket = 0, \quad \llbracket \sigma_{22}(\mathbf{u}_h^0) \rrbracket = 0 \quad \text{on } \mathcal{A}(\llbracket u_{hm}^0 \rrbracket, \lambda_h^0),$$

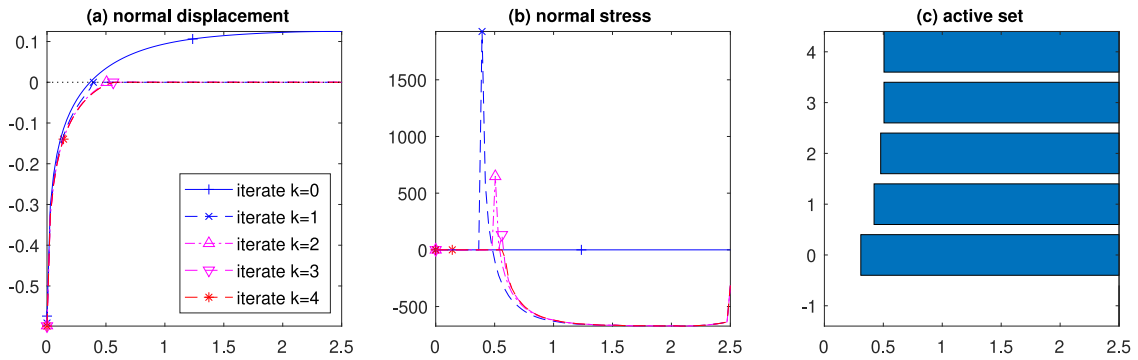


Fig. 11. The solution  $\mathbf{x} + \mathbf{u}_h^0$  of the Signorini contact (a) and symmetric crack problem (b).

whereas the inactive set determines an open crack that is free of stress:

$$\llbracket u_{h1}^0 \rrbracket = 0, \quad \llbracket u_{h2}^0 \rrbracket \geq 0, \quad \llbracket \sigma_{12}(\mathbf{u}_h^0) \rrbracket = 0, \quad \sigma_{22}(\mathbf{u}_h^0) = 0 \quad \text{on } \mathcal{I}(\llbracket u_{hn}^0 \rrbracket, \lambda_h^0).$$

We remark here a smooth closing of the crack faces without the physically inconsistent, square-root singularity.

In this example the issue of stability is tested also with respect to displacement field in the body. For the discretization with  $h = 1/20$  and  $\tau = 1/20$  in two figures we compare maximal amplitude along the contact surface of the horizontal displacement  $\max_{\mathbf{x} \in \Gamma_C^h} (-u_{h1}^m)$  (left) and the vertical displacement  $\max_{\mathbf{x} \in \Gamma_C^h} (-u_{h2}^m)$  (right). They are computed for times  $t^m \in [0, 5]$  [s] within two consequent loops of the forward-backward motion prescribed by (5.2) and (5.3). In Fig. 8 the depicted numerical result by CN evidently oscillates. Whereas in Fig. 9 the spurious oscillations are damped by applying the HHT scheme with  $\alpha = 0.98$  and  $\gamma = 0.6$ ,  $\beta = 0.3025$ .

To solve numerically the mixed variational problem (5.1) we employ the semi-smooth Newton iteration in the form of PDAS Algorithm 4.1, where  $r \in [10^{-8}, 10^8]$ . We demonstrate a typical behavior of the algorithm for the initialization  $\mathcal{A}^{-1} = \emptyset$  at 0-th iterate in Fig. 10. There are about  $10^4$  degrees of freedom in the spatial system as  $h = 1/50$ , and 180 time steps. The contact opening  $U^k$  (left), Lagrange multiplier  $\Lambda^k$  (center), and active set  $\mathcal{A}^k$  (right) are depicted on  $\Gamma_C^h$  with the number  $N_C^h = 90$  of points on discrete contact surface. The algorithm converges in only 5 iterations at the exact solution of the Signorini contact problem (5.1). Typically the iteration number does not exceeded ten for all time steps  $m$ . In this figure we can observe a super-linear convergence of the Newton iterates from Theorem 4.1 and its monotone behavior as stated in Proposition 4.1.

### 6. Conclusion

The semi-smooth Newton method is one of the best iterative algorithms for solution of LCP as well as nonlinear complementarity problems (NLCP) with system matrices which obey the M-property. However, in the larger class of P-matrices this algorithm may cycle [42]. To give more discussion on development of semi-smooth approaches for dynamic contact problems and to present comparisons with other numerical methods known in the literature is the subject of outgoing research.

In the present manuscript, dynamic contact problems for elastic bodies given in multi-domains and domains with cracks are treated in the unified way by FEM semi-discretization and HHT- $\alpha$  methods. For a mixed primal-dual variational formulation of the problem based on Lagrange multipliers, a semi-smooth Newton method converges locally super-linear to the discrete solution. It is equivalent to a primal-dual active set strategy which iterates converge globally monotone, supported by the M-matrix property. The theoretical results are verified in some benchmark experiments carried out for the Signorini contact problem under impact and moving loads.

### Acknowledgments

V.A.K. is supported by the OeAD Scientific & Technological Cooperation (MULT 06/2023) financed by the Austrian Federal Ministry of Science, Research and Economy (BMWF); the autor acknowledges the financial support by the University of Graz. Y.R. is supported by the Ministry for Europe and Foreign Affairs (France) within Programme Danube 2023–2025 (Project PHC Danube n° 49916UM).

### Data availability

No data was used for the research described in the article.

## References

- [1] T.A. Laursen, Computational Contact and Impact Mechanics, Springer, Berlin, 2003, <http://dx.doi.org/10.1007/978-3-662-04864-1>.
- [2] A. Khludnev, V. Kovtunenکو, Analysis of Cracks in Solids, WIT-Press, Southampton, Boston, 2000.
- [3] A.M. Khludnev, J. Sokolowski, Smooth domain method for crack problems, Quart. Appl. Math. 62 (3) (2004) 401–422, <http://dx.doi.org/10.1090/qam/2086037>.
- [4] V.A. Kovtunenکو, Numerical simulation of the non-linear crack problem with non-penetration, Math. Methods Appl. Sci. 27 (2) (2004) 163–179, <http://dx.doi.org/10.1002/mma.449>.
- [5] V.A. Kovtunenکو, Poroelastic medium with non-penetrating crack driven by hydraulic fracture: Variational inequality and its semidiscretization, J. Comput. Appl. Math. 405 (2022) 113953, <http://dx.doi.org/10.1016/j.cam.2021.113953>.
- [6] V.A. Kovtunenکو, N.P. Lazarev, Variational inequality for a Timoshenko plate contacting at the boundary with an inclined obstacle, Phil. Trans. R. Soc. A 382 (2277) (2024) 20230298, <http://dx.doi.org/10.1098/rsta.2023.0298>.
- [7] J. Jarušek, C. Eck, Dynamic contact problems with small Coulomb friction for viscoelastic bodies. Existence of solutions, Math. Models Methods Appl. Sci. 9 (1) (1999) 11–34, <http://dx.doi.org/10.1142/S0218202599000038>.
- [8] O. Chau, A. Heibig, A. Petrov, A class of dynamic unilateral contact problems with sub-differential friction law, in: N. Daras, M. Rassias, N. Zographopoulos (Eds.), Exploring Mathematical Analysis, Approximation Theory, and Optimization, Springer, Cham, 2023, pp. 17–31, [http://dx.doi.org/10.1007/978-3-031-46487-4\\_2](http://dx.doi.org/10.1007/978-3-031-46487-4_2).
- [9] A. Petrov, M. Schatzman, Mathematical results on existence for viscoelastodynamic problems with unilateral constraints, SIAM J. Math. Anal. 40 (5) (2009) 1882–1904, <http://dx.doi.org/10.1137/070695101>.
- [10] T. Kashiwabara, H. Itou, Unique solvability of a crack problem with Signorini-type and Tresca friction conditions in a linearized elastodynamic body, Phil. Trans. R. Soc. A 380 (2236) (2022) 20220225, <http://dx.doi.org/10.1098/rsta.2022.0225>.
- [11] J. Han, L. Lu, S. Zeng, Evolutionary variational-hemivariational inequalities with applications to dynamic viscoelastic contact mechanics, Z. Angew. Math. Phys. 71 (2020) 32, <http://dx.doi.org/10.1007/s00033-020-1260-6>.
- [12] S. Migórski, A. Ochal, M. Shillor, M. Sofonea, Nonsmooth dynamic frictional contact of a thermoviscoelastic body, Appl. Anal. 97 (8) (2018) 1228–1245, <http://dx.doi.org/10.1080/00036811.2017.1344227>.
- [13] H.B. Khenous, P. Laborde, Y. Renard, Mass redistribution method for finite element contact problems in elastodynamics, Eur. J. Mech. A Solids 27 (5) (2008) 918–932, <http://dx.doi.org/10.1016/j.euromechsol.2008.01.001>.
- [14] B. Wohlmuth, Variationally consistent discretization schemes and numerical algorithms for contact problems, Acta Numer. 20 (2011) 569–734, <http://dx.doi.org/10.1017/S0964292911000079>.
- [15] L. Paoli, M. Schatzman, A numerical scheme for impact problems II: The multidimensional case, SIAM J. Numer. Anal. 40 (2) (2002) 734–768, <http://dx.doi.org/10.1137/S003614290037873X>.
- [16] F. Dabaghi, P. Krejčí, A. Petrov, J. Pousin, Y. Renard, A weighted finite element mass redistribution method for dynamic contact problems, J. Comput. Appl. Math. 345 (8) (2019) 338–356, <http://dx.doi.org/10.1016/j.cam.2018.06.030>.
- [17] Y. Ayyad, M. Barboteu, Formulation and analysis of two energy-consistent methods for nonlinear elastodynamic frictional contact problems, J. Comput. Appl. Math. 228 (1) (2009) 254–269, <http://dx.doi.org/10.1016/j.cam.2008.09.024>.
- [18] M. Barboteu, F. Bonaldi, D. Danan, S. El-Hadri, An Improved Normal Compliance method for dynamic hyperelastic problems with energy conservation property, Commun. Nonlinear Sci. Numer. Simul. 123 (2023) 107296, <http://dx.doi.org/10.1016/j.cnsns.2023.107296>.
- [19] F. Chouly, P. Hild, Y. Renard, Finite Element Approximation of Contact and Friction in Elasticity, Birkhäuser, Cham, 2023, <http://dx.doi.org/10.1007/978-3-031-31423-0>.
- [20] F. Chouly, P. Hild, Y. Renard, A Nitsche finite element method for dynamic contact: 1. Space semi-discretization and time-marching schemes, ESAIM: Math. Model. Numer. Anal. 49 (2) (2015) 481–502, <http://dx.doi.org/10.1051/m2an/2014041>.
- [21] F. Chouly, P. Hild, Y. Renard, A Nitsche finite element method for dynamic contact: 2. Stability of the schemes and numerical experiments, ESAIM: Math. Model. Numer. Anal. 49 (2) (2015) 503–528, <http://dx.doi.org/10.1051/m2an/2014046>.
- [22] F. Chouly, R. Mlika, Y. Renard, An unbiased Nitsche's approximation of the frictional contact between two elastic structures, Numer. Math. 139 (3) (2018) 593–631, <http://dx.doi.org/10.1007/s00211-018-0950-x>.
- [23] J. Gwinner, E.P. Stephan, Advanced Boundary Element Methods. Treatment of Boundary Value, Transmission and Contact Problems, Springer, Cham, 2018, <http://dx.doi.org/10.1007/978-3-319-92001-6>.
- [24] G. Bayada, J. Sabil, T. Sassi, Convergence of a Neumann–Dirichlet algorithm for two-body contact problems with non local Coulomb's friction law, ESAIM: Math. Model. Numer. Anal. 42 (2) (2008) 243–262, <http://dx.doi.org/10.1051/m2an:2008003>.
- [25] R.W. Cottle, J.-S. Pang, R.E. Stone, The Linear Complementarity Problem, SIAM, Philadelphia, 1992, <http://dx.doi.org/10.1137/1.9780898719000>.
- [26] T.D. Luca, F. Facchinei, C. Kanzow, Theoretical and numerical comparison of some semismooth algorithms for complementarity problems, Comput. Optim. Appl. 16 (2) (2000) 173–205, <http://dx.doi.org/10.1023/A:1008705425484>.
- [27] J.-P. Dussault, M. Frappier, J.C. Gilbert, Polyhedral Newton-min Algorithms for Complementarity Problems - the Full Report, Research Report, Inria Paris; Université de Sherbrooke, Québec, Canada, 2024, URL: <https://hal.science/hal-04097624>.
- [28] M. Bergounioux, K. Ito, K. Kunisch, Primal-dual strategy for constrained optimal control problems, SIAM J. Control Optim. 37 (4) (1999) 1176–1194, <http://dx.doi.org/10.1137/S0363012997328609>.
- [29] M. Hintermüller, V.A. Kovtunenکو, K. Kunisch, Generalized Newton methods for crack problems with non-penetration condition, Numer. Meth. Partial. Differ. Equ. 21 (3) (2005) 586–610, <http://dx.doi.org/10.1002/num.20053>.
- [30] Y. Renard, Generalized Newton's methods for the approximation and resolution of frictional contact problems in elasticity, Comput. Methods Appl. Mech. Engrg. 256 (2013) 38–55, <http://dx.doi.org/10.1016/j.cma.2012.12.008>.
- [31] M. Hintermüller, V.A. Kovtunenکو, K. Kunisch, Constrained optimization for interface cracks in composite materials subject to non-penetration conditions, J. Eng. Math. 59 (3) (2007) 301–321, <http://dx.doi.org/10.1007/s10665-006-9113-7>.
- [32] M. Hintermüller, V.A. Kovtunenکو, K. Kunisch, A Papkovitch–Neuber-based numerical approach to cracks with contact in 3D, IMA J. Appl. Math. 74 (3) (2009) 325–343, <http://dx.doi.org/10.1093/imatat/hxp017>.
- [33] S. Hartmann, S. Brunssen, E. Ramm, B. Wohlmuth, Unilateral non-linear dynamic contact of thin-walled structures using a primal-dual active set strategy, Internat. J. Numer. Methods Engrg. 70 (8) (2007) 883–912, <http://dx.doi.org/10.1002/nme.1894>.
- [34] S. Abide, M. Barboteu, S. Cherkaoui, S. Dumont, Unified primal-dual active set method for dynamic frictional contact problems, Fixed Point Theory Algorith. Sci. Eng. 2022 (2022) 19, <http://dx.doi.org/10.1186/s13663-022-00729-4>.
- [35] H.M. Hilber, T.J.R. Hughes, R.L. Taylor, Improved numerical dissipation for time integration algorithms in structural dynamics, Earthq. Eng. Struct. Dyn. 5 (3) (1977) 283–292, <http://dx.doi.org/10.1002/eqe.4290050306>.
- [36] H. Huang, N. Pignet, G. Drouet, F. Chouly, HHT- $\alpha$  and TR-BDF2 schemes for dynamic contact problems, Comput. Mech. 73 (5) (2024) 1165–1186, <http://dx.doi.org/10.1007/s00466-023-02405-9>.
- [37] T. Laursen, V. Chawla, Semismooth and semiconvex functions in constrained optimization, Internat. J. Numer. Methods Engrg. 40 (5) (1997) 863–886, [http://dx.doi.org/10.1002/\(SICI\)1097-0207\(19970315\)40:5<3.O.CO>2-V](http://dx.doi.org/10.1002/(SICI)1097-0207(19970315)40:5<3.O.CO>2-V).

- [38] E. Bauer, V.A. Kovtunenکو, P. Krejčí, G.A. Monteiro, L. Paoli, A. Petrov, Modeling the railway track ballast behavior with hypoplasticity, *J. Math. Sci.* (2025) <http://dx.doi.org/10.1007/s10958-025-07602-w>.
- [39] J. Chung, G. Hulbert, A time integration algorithm for structural dynamics with improved numerical dissipation: The generalized- $\alpha$  method, *Trans. ASME, J. App. Mech.* 60 (1993) 371–375, <http://dx.doi.org/10.1115/1.2900803>.
- [40] J.L. Lions, G. Stampacchia, Variational inequalities, *Comm. Pure Appl. Math.* 20 (3) (1967) 493–519, <http://dx.doi.org/10.1002/cpa.3160200302>.
- [41] R. Mifflin, Semismooth and semiconvex functions in constrained optimization, *SIAM J. Control Optim.* 15 (6) (1977) 957–972, <http://dx.doi.org/10.1137/0315061>.
- [42] I.B. Gharbia, J.C. Gilbert, Nonconvergence of the plain Newton-min algorithm for linear complementarity problems with a P-matrix, *Math. Program.* 134 (2) (2012) 349–364, <http://dx.doi.org/10.1007/s10107-010-0439-6>.